PAPER

Check for updates

Synthesis of novel piperazine-based bis(thiazole)(1,3,4-thiadiazole) hybrids as anti-cancer agents through caspase-dependent apoptosis†

Doaa M. Mohamed,[a] Nabila A. Kheder,[a] Marwa Sharaky,[b] Mohamed S. Nafie, [iD] [cd] Kamal M. Dawood [iD] *[a] and Ashraf A. Abbas [iD] *[a]

A series of novel piperazine-based bis(thiazoles) **13a–d** were synthesized in moderate to good yields *via* reaction of the bis(thiosemicarbazones) **7a**, **b** with an assortment of *C*-acetyl-*N*-aryl-hydrazonoyl chlorides **8a–f**. Similar treatment of the bis(thiosemicarbazone) **7a**, **b** with *C*-aryl-*N*-phenylhydrazonoyl chlorides **10a**, **b** afforded the expected bis(thiadiazole) based piperazine products **13b–d** in reasonable yields. Cyclization of **7a**, **b** with two equivalents of α-haloketones **14a–d** led to the production of the corresponding bis(4-arylthiazol)piperazine derivatives **15a–h** in good yields. The structures of the synthesized compounds were confirmed from elemental and spectral data (FTIR, MALDI-TOF, ^{1}H, and ^{13}C NMR). The cytotoxicity of the new compounds was screened against hepatoblastoma (HepG2), human colorectal carcinoma (HCT 116), breast cancer (MCF-7), and Human Dermal Fibroblasts (HDF). Interestingly, all compounds showed promising cytotoxicity against most of the cell lines. Interestingly, compounds **7b**, **9a**, and **9i** exhibited IC$_{50}$ values of 3.5, 12.1, and 1.2 nM, respectively, causing inhibition of 89.7%, 83.7%, and 97.5%, compared to Erlotinib (IC$_{50}$ = 1.3 nM, 97.8% inhibition). Compound **9i** dramatically induced apoptotic cell death by 4.16-fold and necrosis cell death by 4.79-fold. Compound **9i** upregulated the apoptosis-related genes and downregulated the Bcl-2 as an anti-apoptotic gene. Accordingly, the most promising EGFR-targeted chemotherapeutic agent to treat colon cancer was found to be compound **9i**.

1. Introduction

Piperazine has diverse synthetic potential due to the participation of its N1 and N4 atoms in the construction of a huge number of bis-functionalized organic molecules with broad pharmacological applications. Based on statistical analysis, piperazine is the most abundant N-heterocycle after piperidine and pyridine used in developing pharmaceutical small molecule drugs and biomedical materials.[1–6] Piperazine derivatives have emerged as privileged pharmacophores with several therapeutic versatilities.[7–11] In addition, some piperazine-based commercial drugs were approved for cancer treatment, such as Olaparib, Abemaciclib, Palbociclib (breast cancer drugs), Rociletinib (lung cancer drug), and Imatinib (acute lymphoblastic leukemia drug)[12,13] (Fig. 1), and some other approved commercial drugs also employed piperazine moieties such as lorpiprazole (anxiolytic drug), dapiprazole (ophthalmic solutions)[14,15] and piperaquine (antiparasitic drug)[16] (Fig. 1). The piperazine motif has also been found to be an essential part of numerous bioactive natural products.[17,18]

Furthermore, several scientific reports discussed the biological potencies of thiazole-based heterocyclic compounds.[19–23] It was reported that the 1,3-thiazole nucleus had been an integral part of tiazofurin,[24] dasatinib,[25] and dabrafenib[26] (Fig. 2), clinically useful anti-cancer drugs. Furthermore, 1,3,4-thiadiazole derivatives have outstanding pharmacological applications due to their broad spectrum of inhibitory activities, particularly 1,3,4-thiadiazoles, which are of immense significance as potent anti-cancer agents.[27–33] Some marketed anti-cancer FDA-approved drugs were also found to employ the 1,3,4-thiadiazole moiety, such as azeteta, litronesib, and filanesib drugs (Fig. 2).

[a] Department of Chemistry, Faculty of Science, Cairo University, Giza 12613, Egypt. E-mail: kmdawood@sci.cu.edu.eg; ashrafabbas@cu.edu.eg; Fax: +202 35727556; Tel: +202 35676602

[b] Pharmacology Unit, Cancer Biology Department, National Cancer Institute, Cairo University, Cairo, Egypt

[c] Department of Chemistry, College of Sciences, University of Sharjah, P. O. 27272, Sharjah, United Arab Emirates

[d] Department of Chemistry, Faculty of Science, Suez Canal University, Ismailia, 41522, Egypt
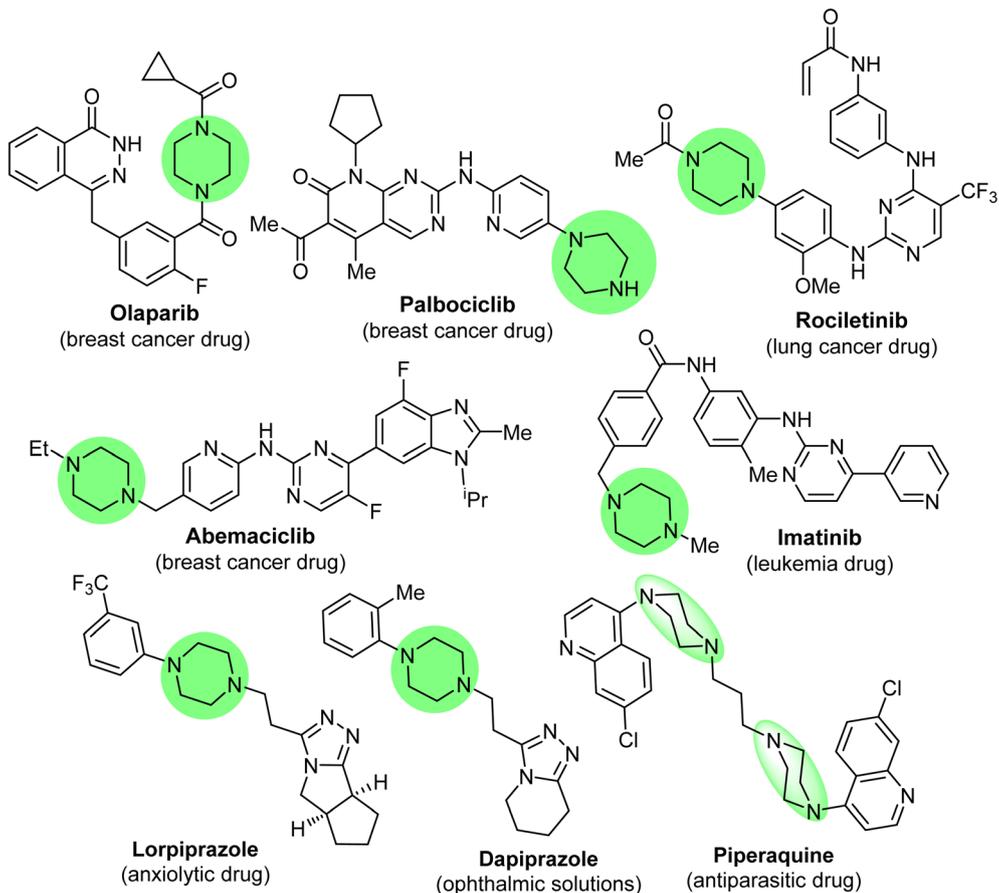
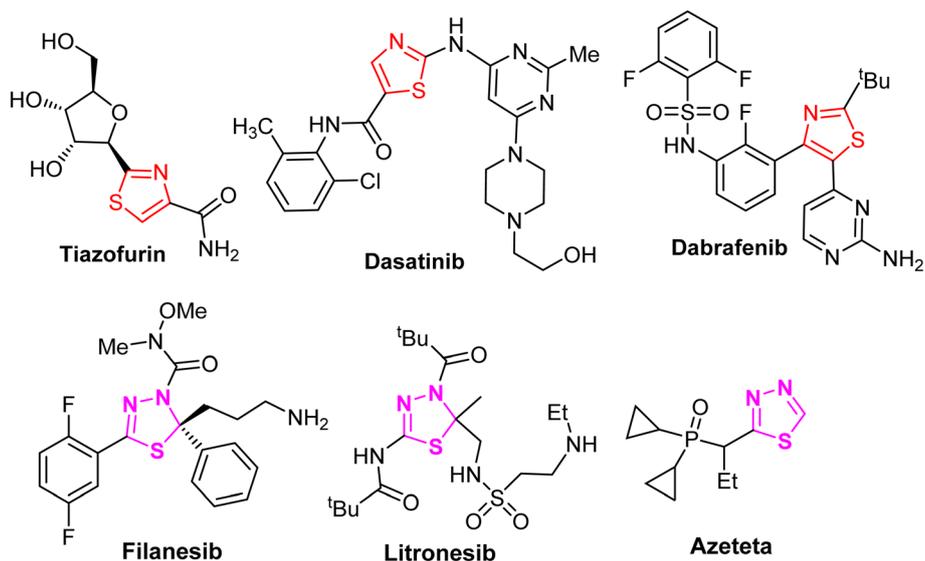Fig. 1 Examples of some piperazine-based marketed drugs.

Fig. 2 Marketed anti-cancer drugs employing thiazole and 1,3,4-thiadiazole motifs.

In addition, organic compounds having bis-carboxamide functionality were found to be components of remarkable biologically active natural products.[34–37] Synthetic bis-carboxamide-based compounds exhibited wide-array inhibitory effects,[38–42] including anti-cancer potencies.[43–45] Bis-carboxamide derivatives were employed as essential constituents of the two
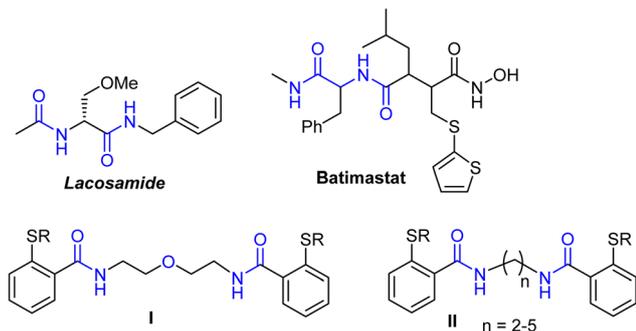
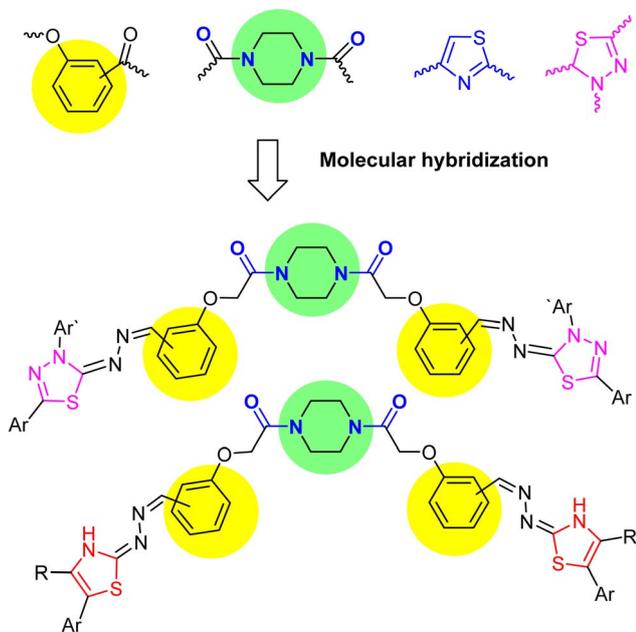Fig. 3 Marketed bis-carboxamide anti-cancer medication.

Fig. 4 Rationale design for molecular hybridization of our targets toward new anti-cancer agents.

marketed drugs, lacosamide and batimastat, and the two anti-cancer agents bis-carboxamides[46] **I** and **II** (Fig. 3).

Recently, our research target has been aimed at building up a wide array of simple- and bis-organic molecules incorporating various heterocyclic nuclei and different functionalities with promising anti-cancer inhibitory activities against numerous human cell lines,[47–57] the reported anti-cancer potencies of compounds employing piperazine, thiazole and/or 1,3,4-thiadiazole, and carboxamide pharmacophores inspired us to synthesize a new library of novel piperazine-based bis-thiazoles and/or thiadiazole hybrids (Fig. 4) having bis-amide linkers. Building on the bis(2-chloroacetamide) derivative **3**, the target compounds were tested for their inhibitory effectiveness as anti-cancer medicines against various cancer cell lines. Additionally, the effective molecular target and apoptotic cell death were investigated.

2.   Results and discussion

2.1.   Chemistry

At first, 1,4-bis(chloroacetyl)piperazine **3** was selected as a key starting material to achieve our goals, as shown in Scheme 1. Thus, reaction of 2 equivalents of chloroacetyl chloride (**1**) with piperazine (**2**) in chloroform at 0 °C afforded compound **3** in a good yield. The reaction of the bis(chloroacetyl) compound **3** with the potassium salts of *ortho-* and *para*-hydoxybenzaldehydes **4a, b** [isolated from treatment of *o*- and *p*-hydoxybenzaldehydes with methanolic KOH solution] in DMF under boiling conditions for 10 min afforded the corresponding 1,4-bis(formylphenoxyacetamido)piperazines **5a, b** in ∼60% yields. In anticipation of the low yield of the previous reaction, the same reaction was repeated using sodium ethoxide as a basic medium instead of KOH/DMF, where the bis-aldehydes **5a, b** were isolated in 71–73% yields.
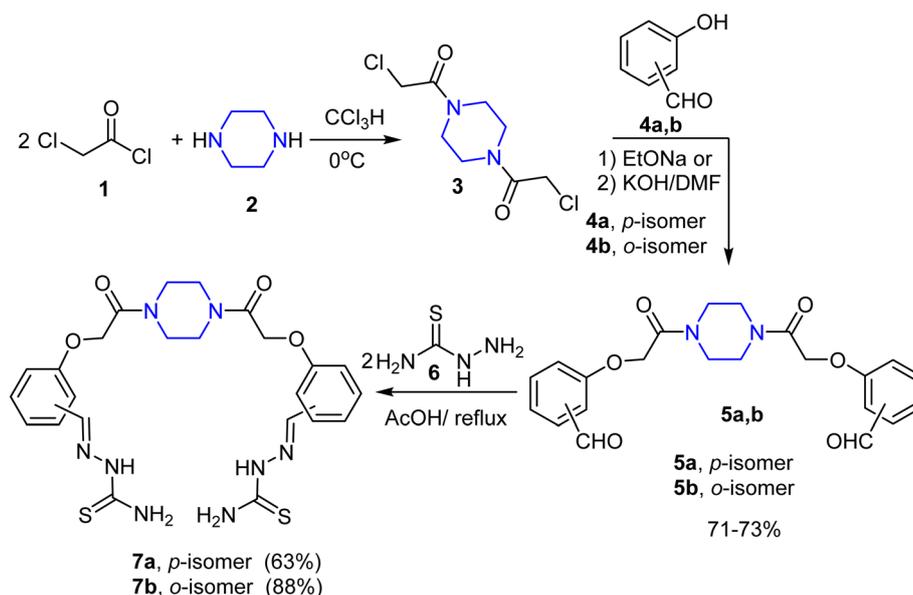
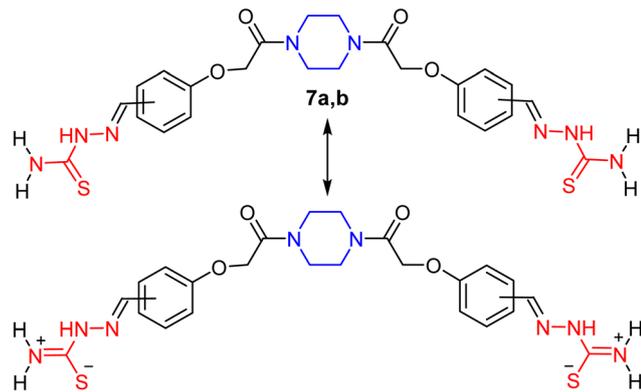Scheme 1 Synthetic route to the bis-thiosemicarbazones 7a, b.

Fig. 5 The tautomeric form of compounds **7a**, **b** with restricted rotation of thioamide group.

The bis-aldehydes **5a**, **b** were then used to construct the novel key starting materials (piperazine-1,4-diyl)bis(hydrazine-1-carbothioamides) **7a**, **b** as depicted in Scheme 1. Therefore, reaction of the bis-aldehydes **5a**, **b** with two equivalents of thiosemicarbazide (**6**) in acetic acid at reflux temperature furnished the novel bis-thiosemicarbazones **7a** and **7b** in 63% and 88% yields, respectively. The structure of the obtained products **7a**, **b** were fully confirmed by both elemental and spectral (IR, ^{1}H NMR, and MALDI-TOF) analyses. The IR spectrum of the

thiosemicarbazone **7a** showed sharp peaks at v 3270, 3439, and 1652 cm^{-1} for NH, NH$_2$, and C=O, respectively. ^{1}H NMR spectrum of **7a** showed characteristic signals for methylene protons of piperazine moiety at δ 3.48–3.54, and a sharp singlet at δ 4.93 assignable to two OCH$_2$ protons, two doublets at δ 6.96 and 7.72 for the *para*-phenylene protons and two singlet signals at δ 7.99 and 11.30 assigned to CH=N, and NH protons, and finally two singlets at δ 7.89 and 8.09 due to the protons of NH$_2$. This is due to the partial double bond character induced by the resonance of the thioamide group as outlined in Fig. 5, which made the germinal protons of amino function electronically non-equivalent. This result is similar to related published studies characteristic of thiosemicarbazone derivatives.[58,59]

The formation of the novel bis(thiosemicarbazones) **7a**, **b** in good yields encouraged us to continue our ongoing interest in the synthesis of some potent biologically active bis(heterocycles). Thus, treatment of the bis-thiosemicarbazone **7a** with 2-oxo-*N*-phenylpropanehydrazonoyl chloride (**8a**)[60] in DMF/ethanol (3 : 1), at reflux temperature, containing two equivalents of triethylamine as a base, afforded the corresponding bis-thiazole derivative **9a** as a single product in 36% yield. The structure of **9a** was fully elucidated by both spectral (IR, ^{1}HNMR, and ^{13}CNMR) as well as elemental analyses and mass spectrometry (*cf.* Experimental section). The IR spectrum of the newly synthesized compound **9a** showed two peaks characteristic for NH and C=O at v 3415 and 1661 cm^{-1}, respectively,
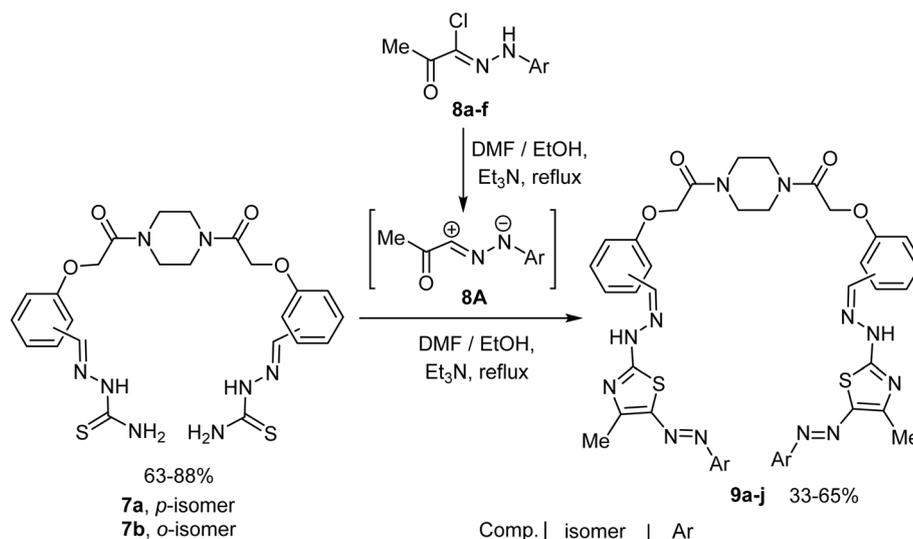
8	Ar
a	C$_6$H$_5$
b	4-MeC$_6$H$_4$
c	4-FC$_6$H$_4$
d	4-ClC$_6$H$_4$
e	4-BrC$_6$H$_4$
f	4-NO$_2$C$_6$H$_4$

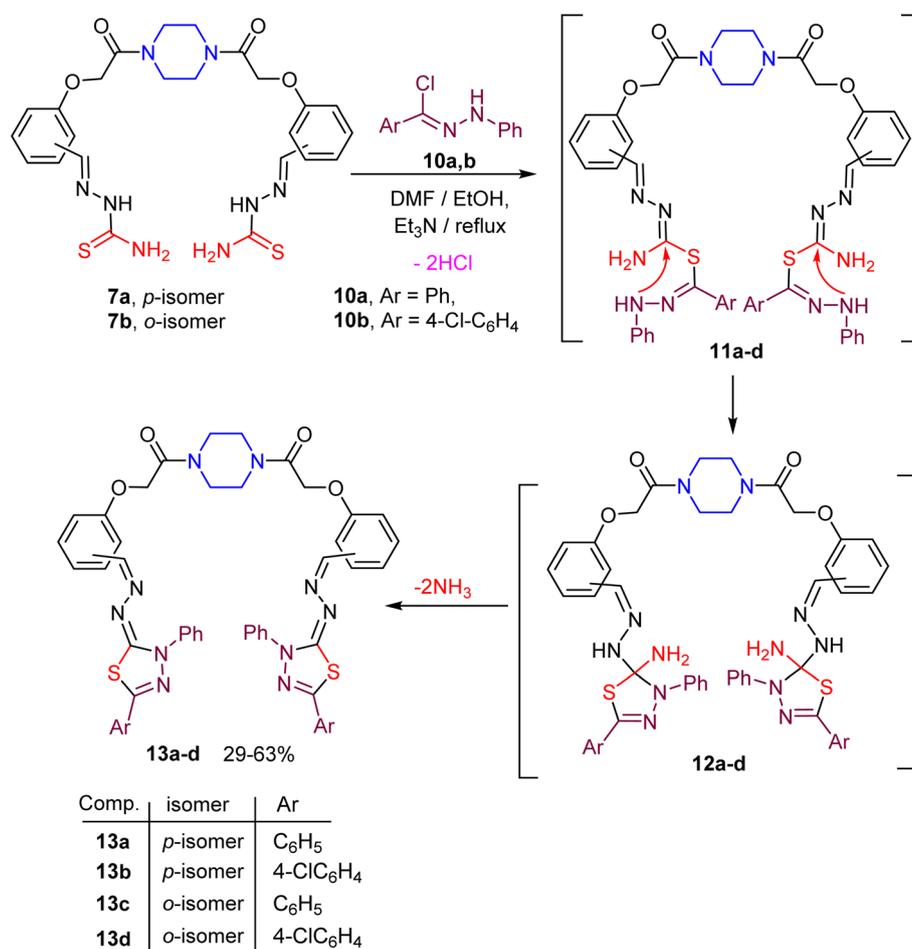| Comp.	isomer	Ar
9a	*p*-isomer	C$_6$H$_5$
9b	*p*-isomer	4-MeC$_6$H$_4$
9c	*p*-isomer	4-FC$_6$H$_4$
9d	*p*-isomer	4-ClC$_6$H$_4$
9e	*p*-isomer	4-NO$_2$C$_6$H$_4$
9f	*o*-isomer	4-MeC$_6$H$_4$
9g	*o*-isomer	4-FC$_6$H$_4$
9h	*o*-isomer	4-ClC$_6$H$_4$
9i	*o*-isomer	4-BrC$_6$H$_4$
9j	*o*-isomer	4-NO$_2$C$_6$H$_4$

Scheme 2 Synthetic route to piperazine-based bis(thiazole) derivatives **9a–j**.

and its ^{1}H NMR spectrum showed the expected features with the appropriate signals, where it revealed three signals at δ 2.59, 3.51–3.57 and 4.99 for the aliphatic protons; two thiazole-methyl groups, four NCH_2 and two OCH_2 groups, respectively, and two singlet signals at δ 8.61 and 10.54 for CH=N, and NH, respectively, in addition to a multiplet in the region δ 7.09–7.83 for the aromatic protons. The ^{13}C NMR spectrum of **9a** showed a total of 17 peaks identified as four peaks at δ 16.43, 40.99, 41.22, 43.80, 44.05 and 65.73 due to aliphatic carbons,[61] and ten peaks at δ 114.12, 115.14, 122.09, 126.68, 129.21, 129.91, 137.87, 143.35, 159.55, 160.81 for the aromatic carbons, besides three peaks at δ 165.64, 171.96, 177.95 for 2C=N and C=O carbons which are compatible with the suggested structure. The positive ion mode MALDI-TOF mass spectrum of **9a** exhibited a molecular ion peak of the form $[M + H]^+$ at m/z = 841.09.
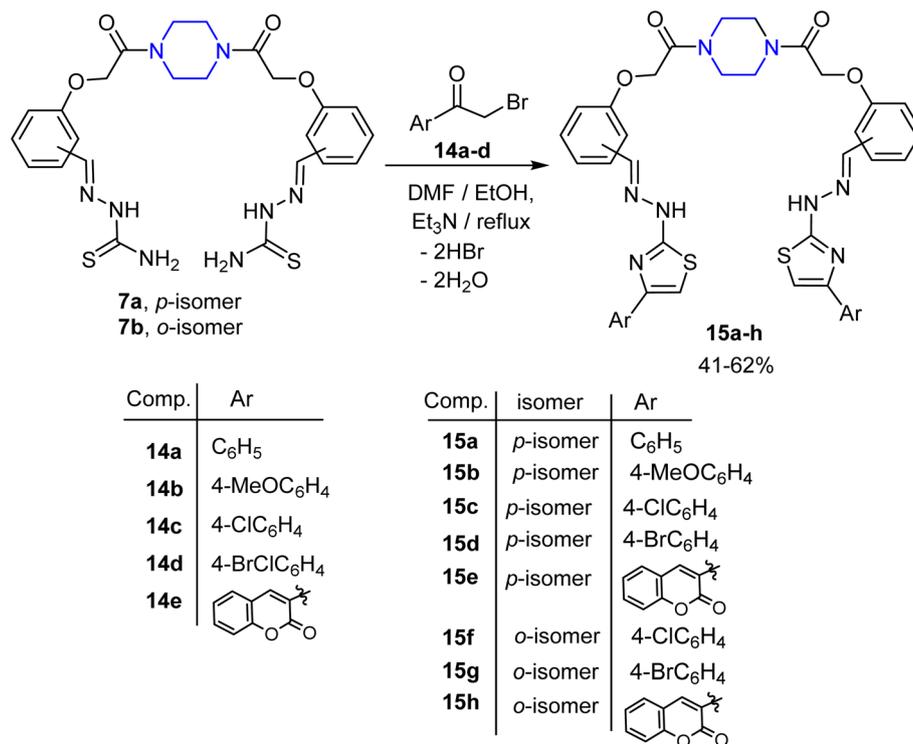
Now, the scope of the last reaction was extended to the bis-thiosemicarbazone **5b** to generate the corresponding bis-thiazole derivatives. Therefore, under typical reaction conditions, the bis-thiosemicarbazones **7a, b** reacted with various hydrazonoyl chlorides **8a–f** (ref. 60, 62 and 63) to afford the corresponding piperazine-based bis(thiazoles) **9b–j** in 33–65% yields. The structures of **9b–j** were enlightened by both elemental and spectral (IR, MALDI-TOF, ^{1}H NMR, and ^{13}C NMR) analyses (*cf.* Experimental section) (Scheme 2).

The next target was aimed to explore the synthetic potential of the piperazine-based bis(thiosemicarbazones) **7a, b** in the construction of the bis(1,3,4-thiadiazole) derivatives **13a–d**. Thus, reaction of the reactive substrate **7a** with *C,N*-diphe-nylhydrazonoyl chloride (**10a**) (ref. 64) in DMF/ethanol mixture containing triethylamine at reflux temperature gave the corresponding bis(1,3,4-thiadiazole) **13a** in 63% yield, as shown in Scheme 3. The structure of compound **13a** was confirmed using spectral data. The absorption band of the imine (C=N) group appeared in the IR spectrum of compound **13a** at ν 1604 cm^{-1}, and the C=O starching band appeared also at ν 1658 cm^{-1}. The ^{1}H NMR spectrum of **13a** showed the existence of multiple signals for the protons of four CH_2N of piperazine moiety at δ 3.50–3.55 as well as a singlet signal for the protons of two OCH_2 linkers at δ 4.95, and a singlet signal at δ 8.43 due to the CH=N function. Furthermore, multiple signals corresponding to the aromatic protons appeared at δ 7.03–8.10. Finally, the mass spectrum of compound **13a** revealed a correct molecular ion peak for $[M + H^+]$ at m/z = 912.32. A similar reaction of the bis(thiosemicarbazone) **7a** with the hydrazonoyl chloride **10b** (ref. 65) gave the corresponding bis(1,3,4-thiadiazole) **13b** in a moderate yield. Under the same reaction conditions, hetero-annulation of the *ortho*-isomeric bis(thiosemicarbazone) **7b** with *N*-arylbenzohydrazonoyl chlorides **10a, b** gave the

Comp.	isomer	Ar
13a	*p*-isomer	C_6H_5
13b	*p*-isomer	$4\text{-}ClC_6H_4$
13c	*o*-isomer	C_6H_5
13d	*o*-isomer	$4\text{-}ClC_6H_4$

Scheme 3 Synthetic route to piperazine-based bis(1,3,4-thiadiazole) hybrids **13a–d**.

Scheme 4 Synthetic route to the piperazine–based bis(thiazol-2-ylidene) derivatives **15a–h**.

anticipated novel piperazine-based bis(1,3,4-thiadiazoles) **13c**, **d** in reasonable yields as depicted in Scheme 3. Formation of the target compounds **13a–d** took place *via* the proposed mechanistic pathway displayed in Scheme 3. Due to the basic condition, the sequential removal of two molecules of hydrochloric acid gave the intermediate **11**, which underwent an intramolecular cyclization to give **12**. Extrusion of two ammonia molecules from the intermediate **12** gave the final product **13**.

Finally, the scope of our approach to synthesize a new series of functionalized piperazine-based bis(thiazol-2-ylidene) derivatives **15a–h** is achieved as shown in Scheme 4. Therefore, under the above reaction conditions, treatment of the bis-thiosemicarbazone **7a** with phenacyl bromide (**14a**)[66] in a 1 : 2 molar ratio led to the production of the corresponding 1,1′-(piperazine-1,4-diyl)bis(2-(4-phenylthiazol-2(3*H*)ylidene-hydrazineylidene)methyl)phenoxy-ethan-1-one (**15a**) as a single product in 48% yield. The ¹H-NMR spectrum of compound **15a** exhibited multiplet peaks in the region δ 3.49–3.56 corresponding to the piperazine protons, and a singlet signal at δ 4.92 for the OCH$_2$ protons, in addition to three singlet peaks at δ 7.3, 7.86, and 11.99 assigned for the protons of thiazole-5-CH, imine (CH=N), and NH, respectively. The ¹³C NMR spectrum displayed five aliphatic carbon atoms at δ 41.18, 41.40, 44.03, 44.53, and 66.03 assigned to the CH$_2$'s of piperidine moiety and OCH$_2$ linker, ten aromatic carbon atoms at δ 94.41, 103.49, 115.18, 125.61, 127.53, 127.75, 128.71, 134.83, 141.25, and 150.60 in addition to three signals at δ 159.12, 166.02 and 168.45 assigned to two C=N and C=O carbons.

Table 1 Percentage of cell growth inhibition at the single dose [100 μM] for the tested compounds against HCT116, HEPG2, MCF7 and HDF cell lines

| Comp.	Percentage of cell growth inhibition at [100 μM]			
	HCT116	HEPG2	MCF7	HDF
7a	86.23 ± 5.33	83.30 ± 7.47	85.29 ± 5.20	45.09 ± 30.14
7b	90.07 ± 3.41	89.13 ± 2.22	88.90 ± 5.46	66.45 ± 11.48
9a	81.00 ± 3.91	74.72 ± 4.49	85.88 ± 5.94	18.16 ± 11.54
9b	85.16 ± 2.11	56.50 ± 4.93	89.48 ± 2.34	27.57 ± 25.06
9c	87.20 ± 4.53	77.19 ± 3.10	90.27 ± 1.30	67.68 ± 11.53
9d	89.11 ± 2.04	73.11 ± 5.28	90.45 ± 1.99	57.72 ± 17.99
9e	86.85 ± 2.09	77.52 ± 7.73	84.60 ± 2.019	18.59 ± 32.06
9f	85.36 ± 6.41	93.45 ± 2.072	85.53 ± 2.11	78.32 ± 3.64
9g	80.64 ± 7.04	91.80 ± 3.29	88.68 ± 4.11	71.06 ± 21.58
9h	77.71 ± 8.59	83.97 ± 3.07	81.05 ± 7.44	55.95 ± 23.63
9i	89.61 ± 5.30	90.95 ± 3.56	89.87 ± 2.30	71.60 ± 17.26
9j	87.68 ± 4.30	83.09 ± 7.22	71.40 ± 20.50	12.01 ± 6.04
13a	78.07 ± 5.78	71.42 ± 4.92	88.25 ± 1.88	52.49 ± 14.75
13b	89.34 ± 2.83	85.14 ± 3.16	90.81 ± 1.39	79.15 ± 3.71
13c	76.41 ± 5.38	68.83 ± 12.69	86.16 ± 1.83	60.79 ± 3.0939
13d	88.87 ± 1.38	80.02 ± 3.39	86.37 ± 2.56	64.02 ± 10.80
15a	78.09 ± 6.50	67.93 ± 7.03	87.26 ± 1.63	50.19 ± 21.51
15b	21.75 ± 16.49	83.39 ± 9.48	50.64 ± 10.22	48.00 ± 48.46
15c	53.11 ± 19.55	42.58 ± 11.48	82.42 ± 1.15	40.60 ± 13.65
15d	74.82 ± 0.38	62.26 ± 18.32	89.20 ± 1.59	58.44 ± 25.12
15e	73.88 ± 4.08	74.44 ± 4.88	68.37 ± 7.33	68.13 ± 10.09
15f	63.59 ± 5.34	71.19 ± 3.61	75.98 ± 10.50	66.86 ± 12.10
15g	61.76 ± 8.01	74.828 ± 2.18	71.29 ± 11.94	54.76 ± 21.19
15h	36.44 ± 13.81	70.12 ± 8.68	46.72 ± 11.33	44.00 ± 51.49
DOX	82.77 ± 2.98	89.09 ± 0.63	86.37 ± 1.82	30.53 ± 9.75
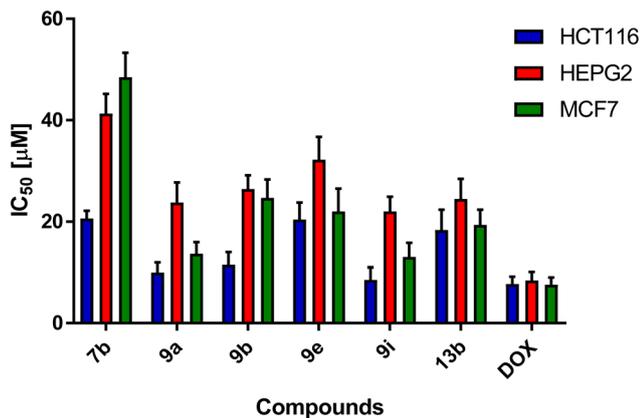
Fig. 6 Cytotoxicity of selected compounds on HCT116, HEPG2, and MCF7 cell lines after 48 h treatment by sulphorhodamine assay. Graphs and data analysis were performed using GraphPad InStat, version 8.

Table 2 IC_{50} values of **7b**, **9a**, **9b**, **9e**, **9i** and **13b** on HCT116, HEPG2, MCF7 and HDF cell lines

| Comp. | IC_{50} (μM) $\pm$ SD | | |
	HCT116	HEPG2	MCF7
7b	20.66 ± 1.5	41.3 ± 3.9	48.5 ± 4.8
9a	9.98 ± 2	23.78 ± 4	13.67 ± 2.3
9b	11.5 ± 2.5	26.46 ± 2.7	24.73 ± 3.6
9e	20.40 ± 3.4	32.2 ± 4.5	22.01 ± 4.5
9i	8.51 ± 2.5	22.02 ± 2.9	13.01 ± 2.8
13b	18.36 ± 4	24.49 ± 4	19.38 ± 3
DOX	7.7 ± 1.5	8.42 ± 1.7	7.59 ± 1.4

The above reaction was generalized by applying a typical procedure for the reaction of bis-thiosemicarbazones **7a, b** with different reactive synthons of the α-bromoketones **14b–e** (ref. 67 and 68). The reaction proceeded straightforwardly and produced the corresponding piperazine-based bis((4-arylthiazol-2-ylidene)hydrazono) derivatives **15b–h** in moderate to good yields, as shown in Scheme 4. Spectroscopic data and elemental analyses were used to establish the constitution of the targeted compounds **15a–h** (see experimental data).

Table 3 IC_{50} values of EGFR kinase inhibition of the most cytotoxic compounds

Compound	% of EGFR inhibition	$IC_{50} \pm SD^{a}$ (nM)
7b	89.7 ± 2.8	3.5 ± 0.1
9a	83.7 ± 1.4	12.1 ± 0.04
9b	74.8 ± 1.6	54.6 ± 0.9
9i	97.5 ± 2.1	1.2 ± 0.05
Erlotinib	97.8 ± 2.8	1.3 ± 0.01

[a] "Values are expressed as an average of three independent replicates". "IC_{50} values were calculated using sigmoidal non-linear regression curve fit of percentage inhibition against five concentrations of each compound".

2.2. Biological evaluation

2.2.1. Cytotoxic activity. Anti-cancer activity of the synthesized compounds was assessed against hepatoblastoma (HepG2), human colorectal carcinoma (HCT 116), breast cancer (MCF-7), and Human Dermal Fibroblasts (HDF) cell lines. Sulforhodamine B colorimetric assay was used for cytotoxicity screening.[69,70]

The effect of the addition of different concentrations of the newly synthesized compounds on HCT-116, HEPG2, MCF7, and HDF cell lines was examined. All the synthesized compounds were used in single-dose 100 μM for 48 h on HCT116, HEPG2, MCF7, and HDF cell lines as described in Table 1. Interestingly, compounds **7b**, **9a**, **9b**, **9e**, **9i**, and **13b** showed potent percentage of cell growth inhibition on the cancer cell lines exceeding 80% with low percentage against normal cells, and hence, they were employed in measuring their IC_{50} values, where the extent of cytotoxicity of the selected compounds on cancer cell lines was significantly prominent. This resulted in a marked inhibition in the cellular proliferation of cancer cell lines in 100 μM concentration, as presented in Table 1 and Fig. 6. Compound **9i** exhibited the most potent inhibitory activity against HCT116, HEPG2, and MCF7 cancer cells with IC_{50} values of 8.51 ± 2.5, 22.02 ± 2.9, and 13.01 ± 2.8 μM, respectively. Additionally, compound **9a** exhibited potent cytotoxicity against HCT116, HEPG2 and MCF7 with IC_{50} values of 9.98 ± 2, 23.78 ± 4 and 13.67 ± 2.3 μM, respectively (Table 2).

2.2.2. EGFR kinase inhibitory assay. Compounds **7b**, **9a**, **9b**, and **9i** were tested for their inhibitory effects against EGFR to determine their molecular targets. Regarding cytotoxicity against HCT-116 cells, these substances ranked first. As seen in Table 3, the tested compounds showed promising EGFR kinase inhibition activity; interestingly, compounds **7b**, **9a**, and **9i** exhibited IC_{50} values of 3.5, 12.1, and 1.2 nM, respectively, causing inhibition of 89.7%, 83.7%, and 97.5%, compared to Erlotinib (IC_{50} = 1.3 nM, 97.8% inhibition). Compound **9b** exhibited moderate EGFR inhibition with an IC_{50} value of 54.6 nM with inhibition activity of 74.8%. Therefore, the ability of compound **9i** to inhibit EGFR kinase and trigger apoptotic cell death in HCT-116 cells was investigated.

2.2.3. Apoptotic investigation

2.2.3.1. Annexin V/PI staining with cell cycle analysis. Using flow cytometric examination of Annexin V/PI staining, the apoptotic cell death in both untreated and treated HCT-116 cells was investigated to assess the apoptotic activity of compound **9i** (IC_{50} = 8.5 μM, 48 h). Fig. 7A showed that compound **9i** significantly induced apoptotic cell death; it induced total apoptosis by 16.85% (16.31% for late apoptosis, 0.54% for early apoptosis) compared to the untreated control group (2.36% for late apoptosis, 1.69% for early apoptosis). Additionally, it induced necrosis cell death by 4.79-fold, and it induced necrosis by 35.74% compared to 7.45% in the untreated control.

Next, DNA flow cytometry was used to estimate the cell population in each cell phase following treatment with cytotoxic agents. As seen in Fig. 7B, compound **9i** treatment increased the cell population at the P2 phase by 51.89% compared to control 3.77%. Compound **9i** caused cell death in HCT-116 cells, stopping their growth in the P2 phase which represent the apoptosis cell death.
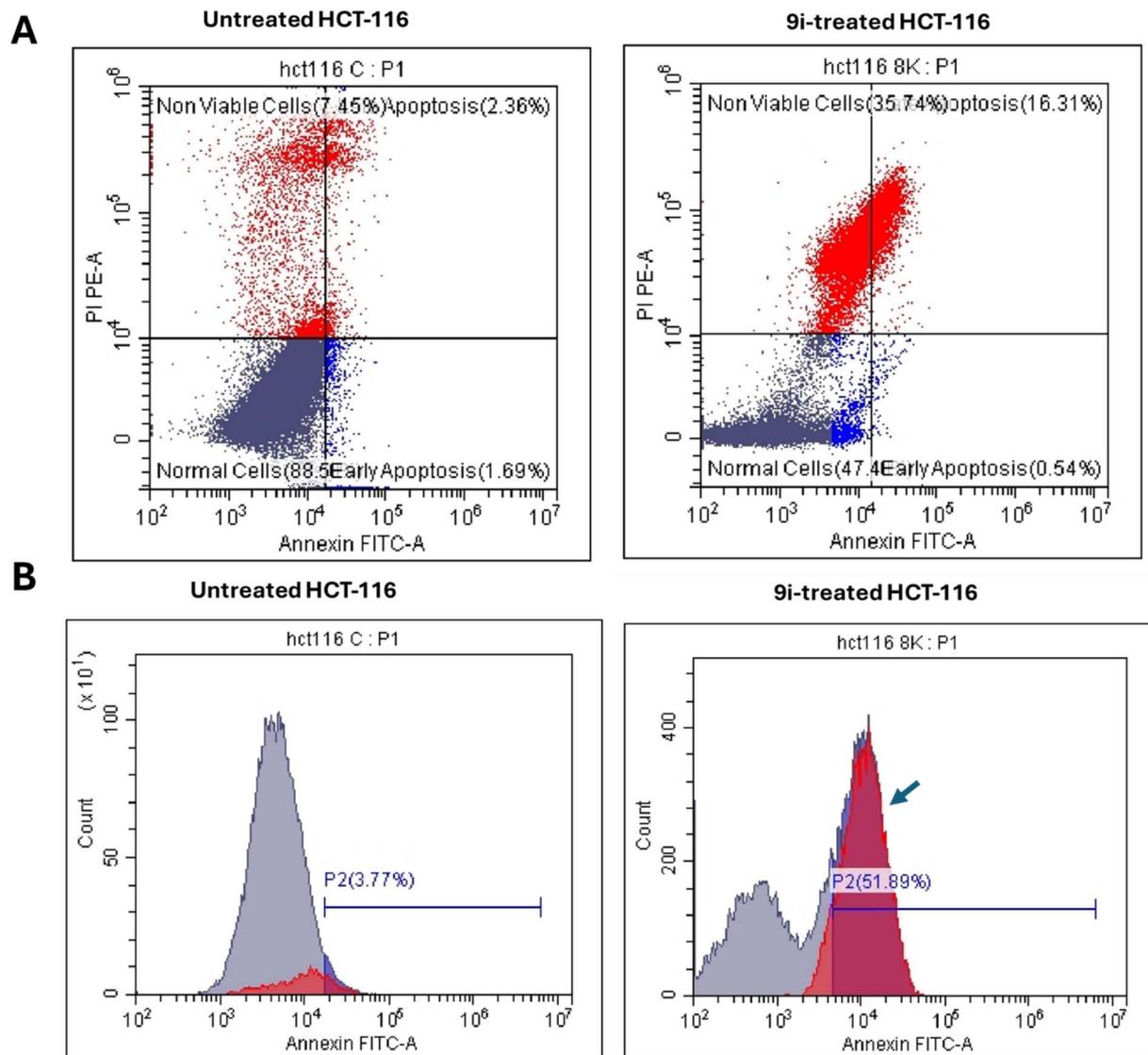
Fig. 7 (A) Cryptographs of Annexin-V/propidium iodide staining of untreated and **9i**-treated HCT-116 cells with (IC_{50} = 8.5 μM, 48 h). (B) Percentage of cell population at each cell cycle "G1, and G2" using DNA content-flow cytometry aided cell cycle analysis. Cell arrest happened at the P2 phase (arrow indicated).

2.2.3.2. RT-PCR. It was determined by comparing the RT-PCR levels of apoptosis-mediated genes P53, bax, caspase-3,8,9, and Bcl-2 in the untreated and treated HCT-116 cells, compound **9i** induced apoptotic cell death in these cells. As seen in Fig. 8, compound **9i** upregulated caspase-3,8,9 levels by 9.87, 7.6, and 11.6-fold change, PUMA by 8.5-fold change, and P53 by 10.87-fold change, while it downregulated the Bcl-2 expression by 0.76-fold change. The results showed that compound **9i** administration triggered cell death by apoptosis through intrinsic and extrinsic pathways.

3. Experimental

3.1. Chemistry

3.1.1. General part. All melting points were measured on a Gallenkamp melting point apparatus and were uncorrected. The infrared spectra (IR) were recorded in potassium bromide disks on pye Unicam SP 3300 and Shimadzu FT IR 8101 PC infrared spectrophotometers (Pye Unicam Ltd Cambridge, England and Shimadzu, Tokyo, Japan, respectively). The NMR spectra were recorded on Varian Mercury Vx-300 BB (running at 300 MHz for ^{1}H) (Microanalytical Unit, Cairo University, Egypt) equipment. The spectra were obtained from deuterated DMSO and the chemical shifts were reported in ppm units downfield from tetramethylsilane (TMS) as an internal standard. Elemental analyses were performed at the Microanalytical Center, Cairo University, Giza, Egypt. The hydrazonoyl halides **8a–f**,[60,62,63] **10a, b**,[64,65] and α-bromoketones **14a–d** (ref. 66–68) were synthesized following the literature procedures. Anticancer evaluations were conducted at the National Cancer Institute, Cairo University, Giza, Egypt. Some products were fairly soluble in NMR solvents and their ^{13}C NMR could not be measured.
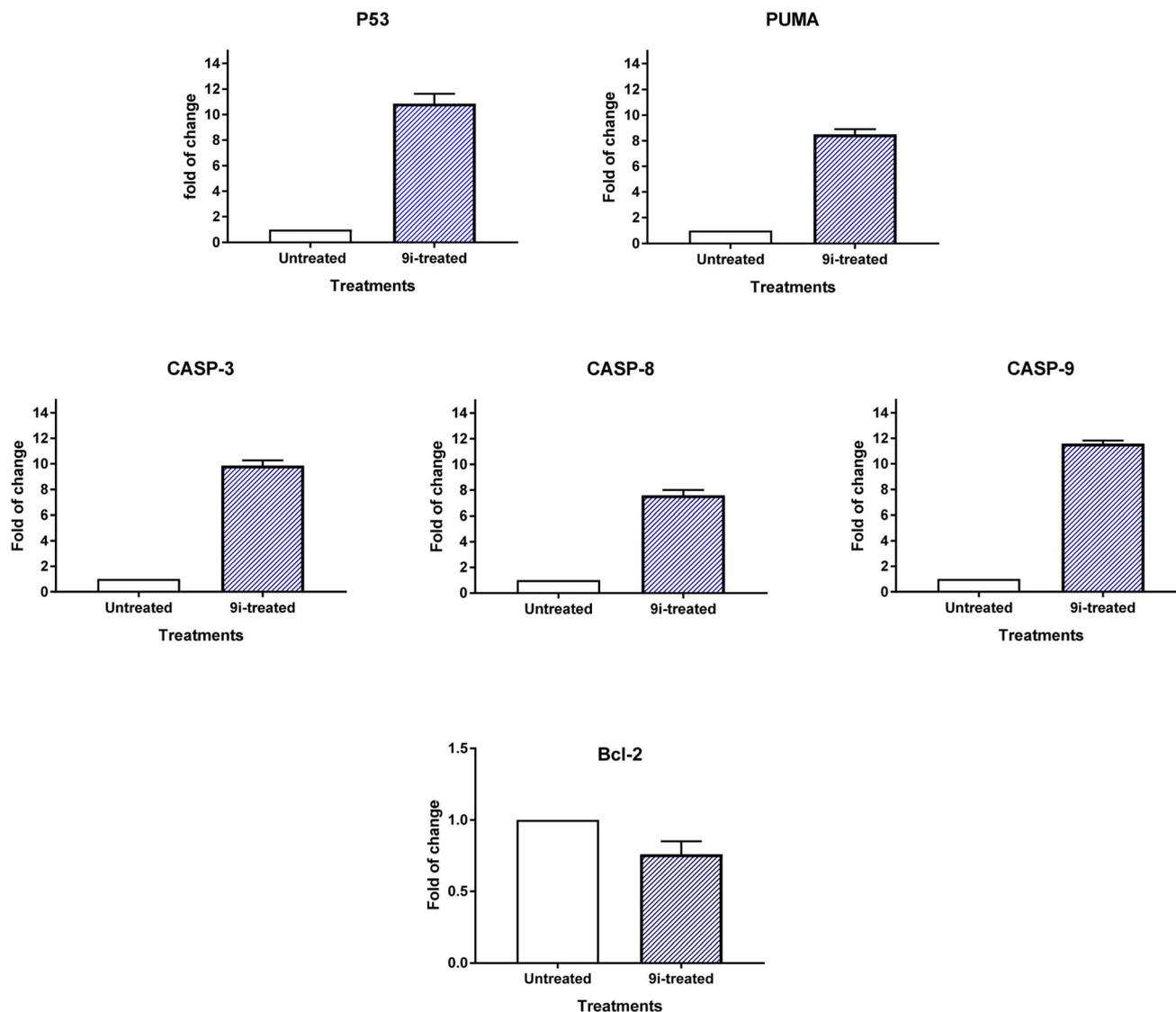
Fig. 8 Quantitative RT-PCR results analysis of the apoptosis-related genes; P53, bax, caspases 3, 8, 9, and Bcl-2, respectively in HCT-116 cells treated with compound **9i** with (IC_{50} = 8.5 μM, 48 h). The data illustrated is the average of 3 independent experimental runs (mean ± SD). Fold change of untreated control = 1.

3.1.1.1 Molecular weight determination using MALDI-TOF/ MS. Matrix-assisted Laser Desorption Ionization Time-of-flight mass spectrometry (MALDI-TOF/MS) (Bruker, model ultra-FlexXtreme) was used to determine the molecular weight of the new products. The measurements were examined in positive mode using a reflectron time-of-flight mass spectrometer. The instrument was calibrated with a peptide calibration standard. The sample was prepared as follows: the matrix DCTB dissolved in tetrahydrofuran (THF) (DCTB = *trans*-2-3-(4-*tert*-butylphenyl)-2-(methyl-2-propenylidene)malononitrile ≥99.0%) was purchased from Sigma. All samples were dissolved in THF. The samples were deposited on the target plate as follows: 2 μL of the sample was mixed with 2 μL of the matrix solution in a 1 : 1 ratio using an Eppendorf Research Plus micropipette. Using a micropipette, a single drop of the solution mixture was placed

on a specific labeled location in the target plate and then allowed to dry at room temperature.

3.1.2. Synthesis of the bis-benzaldehyde derivatives 5a, b

3.1.2.1 Method A. Potassium hydroxide (1.14 g, 20 mmol) was dissolved in methanol (10 mL), then the resulting solution was mixed with *p*- or *o*-hydroxybenzaldehyde derivatives **4a, b** (2.44 g, 20 mmol). The resulting mixtures were stirred at ambient temperature for 10 min. Then the solvent was evaporated under reduced pressure. The obtained potassium salts were treated with dry ether and involved in the next step as crude materials. Dissolving potassium salts (20 mmol) in dimethylformamide (15 mL), then adding the bis(dichloro) compound **3** (10 mmol) and leaving the reaction mixture to boil at reflux for 10 min, potassium chloride was extruded. After that, the reaction solvent was evaporated and the precipitated materials were collected and washed with water. The isolated

solid products obtained were purified by recrystallization from the ethanol/acetic acid to produce the corresponding bis(aldehyde) derivatives **5a, b** in about 60% yield.[71]

3.1.2.2 Method B. p- or o-hydroxybenzaldehydes **4a** or **4b** (2.44 g, 20 mmol) was added to sodium ethoxide solution [prepared from sodium (0.5 g, 20 mmol) in dry ethyl alcohol (30 mL)]. The product mixture was heated at reflux temperature for 10 min., then the bis(dichloro) derivative **3** (10 mmol) was added. The reaction mixture was heated at reflux condition for 4 h. The solvent was then evaporated under reduced pressure, and the remaining solid products were washed with cold water. The solid obtained was collected and purified by recrystallization from ethanol/acetic acid to give the bis(aldehyde) derivatives **5a, b** in about 72% yield.

3.1.3. Synthesis of the bis-thiosemicarbazone derivatives 7a, b

3.1.3.1 General procedure. The appropriate bis-aldehydes **5a** or **5b** (2.05 g, 5 mmol) were dissolved in acetic acid (20 mL), then thiosemicarbazide (**6**) (0.91 g, 10 mmol) was added and the produced mixture was refluxed for 1 h with stirring. The reaction contents were left to cool to ambient temperature and the produced solid material was collected by filtration, washed with ethanol, and dried. Purification of the products by recrystallization from DMF/EtOH (1 : 1 v/v) gave the corresponding bis-thiosemicarbazone derivatives **7a, b.**

3.1.3.2 1,1′-(Piperazine-1,4-diyl)bis(2-(4-(2-carbamothioylhydrazono)methylphenoxy)ethanone) (7a). Pale yellow crystals, 0.85 g (yield 63%). Mp 236–238 °C; IR (KBr) ν 3270, 3439 (NH, NH$_2$), 1652 (C=O), 1243 (C=S) cm^{-1}; MS: MALDI-TOF: calcd for [M + H]$^+$ m/z = 557.66, found 557.33; ^{1}H NMR (DMSO-d$_6$) δ 3.48–3.54 (m, 8H, 4N–CH$_2$), 4.93 (s, 4H, 2OCH$_2$), 6.96 (d, J = 8.7 Hz, 4H, ArH's), 7.72 (d, J = 8.4 Hz, 4H, ArH's), 7.89, 8.09 (2 s, 4H, 2NH$_2$), 7.99 (s, 2H, CH=N), 11.30 (s, 2H, 2NH); Anal. calcd: for C$_{24}$H$_{28}$N$_8$O$_4$S$_2$ (556.66): C, 51.78; H, 5.07; N, 20.13%. Found: C, 51.60; H, 4.78; N, 20.30%.

3.1.3.3 1,1′-(Piperazine-1,4-diyl)bis(2-(2-(2-carbamothioylhydrazono)methylphenoxy)ethanone) (7b). Pale yellow crystals, 1.2 g (yield 88%). Mp 230–232 °C; IR (KBr) ν 3286, 3387 (NH, NH$_2$), 1670 (C=O), 1253 (C=S) cm^{-1}; MS: MALDI-TOF: calcd for [M + H]$^+$ m/z = 557.66, found 557.43; ^{1}H NMR (DMSO-d$_6$) δ 3.52–3.55 (m, 8H, 4 NCH$_2$), 4.96 (s, 4H, 2OCH$_2$), 6.94–7.0 (m, 4H, ArH's), 7.34 (t, J = 8.4 Hz, 2H, ArH's), 7.94 (s, 2H, 2 NH), 8.07–8.01 (m, 4H, 2 NH & 2 ArH's), 8.45 (s, 2H, 2CH=N), 11.47 (s, 2H, 2 NH) ppm; ^{13}C NMR (DMSO-d$_6$) δ 41.06, 41.45, 44.08, 44.47, 66.31, 112.79, 120.99, 122.46, 126.33, 131.05, 138.04, 156.52, 165.91, 177.87 ppm; Anal. calcd: for C$_{24}$H$_{28}$N$_8$O$_4$S$_2$ (556.66): C, 51.78; H, 5.07; N, 20.13%. Found: C, 51.84; H, 5.12; N, 20.02%.

3.1.4. Synthesis of piperazine-based bis-thiazole hybrids 9a–j and bis-1,3,4-thiadiazoles 13a–d

3.1.4.1 General procedure. A mixture of the appropriate bis-thiosemicarbazones **7a, b** (0.5 mmol, 0.265 g) and the appropriate N-aryl-hydrazonoyl chlorides **8a–f** or **12a, b** (1 mmol) in absolute ethanol/DMF (1 : 3, 10 mL), was refluxed for 6–8 hours in the presence of triethylamine (0.1 mL). The reaction vessel was left to cool to ambient temperature and the isolated solid product was collected by filtration, washed with ethanol, and

dried. The dried products were then purified by recrystallization from DMF/EtOH mixture to give the targeted bis-(1,3-thiazoles) **9a–j** or bis-(1,3,4-thiadiazoles) **13a–d**, respectively.

3.1.4.2 1,1′-(Piperazine-1,4-diyl)bis(2-(4-(((4-methyl-5-(phenylazo)thiazol-2-yl)hydrazono)methyl)-phenoxy)ethanone) (9a). Orange crystals, yield (0.11 g, 36%), mp 180–182 °C: IR (KBr) ν 3415 (NH), 1661 (C=O) cm^{-1}; MS: MALDI-TOF: calcd for [M + H]$^+$ m/z = 841.98, found 841.09; ^{1}H NMR (DMSO-d$_6$) δ 2.59 (s, 6H, 2CH$_3$), 3.51–3.57 (m, 8H, 4 NCH$_2$), 4.99 (s, 4H, 2OCH$_2$), 6.98 (t, J = 6.9 Hz, 4H, ArH's), 7.09 (d, J = 8.4 Hz, 4H, ArH's), 7.30–7.38 (m, 6H, ArH's), 7.83 (d, J = 8.4 Hz, 4H, ArH's), 8.61 (s, 2H, 2CH=N), 10.54 (s, 2H, 2 NH); ^{13}C NMR (DMSO-d$_6$) δ 16.43, 40.99, 41.22, 43.80, 44.05, 65.73, 114.12, 115.14, 122.09, 126.68, 129.21, 129.91, 137.87, 143.35, 159.55, 160.81, 165.64, 171.96, 177.95. Anal. calcd: for C$_{42}$H$_{40}$N$_{12}$O$_4$S$_2$ (840.98): C, 59.98; H, 4.79; N, 19.99%. Found: C, 59.75; H, 4.90; N, 20.03%.

3.1.4.3 1,1′-(Piperazine-1,4-diyl)bis(2-(4-(((4-methyl-5-(4-tolylazo)thiazol-2-yl)hydrazono)methyl)-phenoxy)ethanone) (9b). Orange crystals, yield (0.2 g, 65%), mp 192–194 °C: IR (KBr) ν 3421 (NH), 1652 (C=O) cm^{-1}; MS: MALDI-TOF: calcd for [M + H]$^+$ m/z = 870.04, found 871.25; ^{1}H NMR (DMSO-d$_6$) δ 2.26 (s, 6H, 2CH$_3$Ar), 2.57 (s, 6H, 2CH$_3$), 3.51–3.57 (m, 8H, 4CH$_2$N), 4.99 (s, 4H, 2OCH$_2$), 7.08–7.15 (m, 8H, ArH's), 7.26 (d, J = 7.5 Hz, 4H, ArH's), 7.82 (d, J = 7.2 Hz, 4H, ArH's), 8.59 (s, 2H, 2CH=N), 10.49 (s, 2H, 2 NH) ppm; ^{13}C NMR (DMSO-d$_6$) δ 16.57, 20.48, 41.10, 41.60, 43.89, 44.15, 65.85, 114.28, 115.28, 126.85, 129.59, 130.02, 131.30, 137.36, 141.17, 159.52, 160.91, 165.80, 172.19, 177.93 ppm. Anal. calcd: for C$_{44}$H$_{44}$N$_{12}$O$_4$S$_2$ (869.04): C, 60.81; H, 5.10; N, 19.34%. Found: C, 60.75; H, 4.95; N, 19.23%.

3.1.4.4 1,1′-(Piperazine-1,4-diyl)bis(2-(4-(((4-methyl-5-(4-fluorophenylazo)thiazol-2-yl)hydrazono)-methyl)phenoxy) ethanone) (9c). Orange crystals, yield (0.16 g, 52%), mp 210–212 °C; IR (KBr) δ 3422 (NH), 1662 (C=O) cm^{-1}; MS: MALDI-TOF: calcd for [M + K]$^+$ m/z = 915.96, found 915.24; ^{1}H NMR (DMSO-d$_6$) δ 2.58 (s, 6H, 2CH$_3$), 3.51–3.57 (m, 8H, 4 CH$_2$ N), 4.99 (s, 4H, 2OCH$_2$), 7.09 (d, J = 8.4 Hz, 4H, ArH's), 7.17 (t, J = 8.4, 4H, ArH's) 7.34–7.38 (m, 4H, ArH's), 7.82 (d, J = 8.4 Hz, 4H, ArH's), 8.61 (s, 2H, 2CH=N), 10.55 (s, 2H, 2 NH) ppm; ^{13}C NMR (DMSO-d$_6$) δ 16.40, 40.21, 40.98, 43.54, 44.04, 65.76, 115.40, 115.51, 115.75, 116.05, 126.66, 129.92, 137.89, 139.95, 159.59, 160.82, 165.65, 171.86, 177.94 ppm. Anal. calcd: for C$_{42}$H$_{38}$F$_2$N$_{12}$O$_4$S$_2$ (876.96): C, 57.52; H, 4.37; N, 19.17%. Found: C, 57.65; H, 4.15; N, 19.25%.

3.1.4.5 1,1′-(Piperazine-1,4-diyl)bis(2-(4-(((4-methyl-5-(4-chlorophenylazo)thiazol-2-yl)hydrazono)-methyl)phenoxy) ethanone) (9d). Pale brown crystals, yield (0.21 g, 63%), mp 220–222 °C; IR (KBr) ν 1662 (C=O) cm^{-1}; MS: MALDI-TOF: calcd for [M + H]$^+$ m/z = 910.87, found 910.90; ^{1}H NMR (DMSO-d$_6$) δ 2.58 (s, 6H, 2CH$_3$), 3.50–3.56 (m, 8H, 4CH$_2$N), 4.99 (s, 4H, 2OCH$_2$), 7.09 (d, J = 8.1 Hz, 4H, ArH's), 7.36 (s, 8H, ArH's), 7.81 (d, J = 8.7 Hz, 4H, ArH's), 8.61 (s, 2H, 2CH=N), 10.61 (s, 2H, 2 NH). Anal. calcd: for C$_{42}$H$_{38}$Cl$_{12}$N$_{12}$O$_4$S$_2$ (909.87): C, 55.44; H, 4.21; N, 18.47%. Found: C, 55.62; H, 4.25; N, 18.22%.

3.1.4.6 1,1′-(Piperazine-1,4-diyl)bis(2-(4-(((4-methyl-5-(4-nitrophenylazo)thiazol-2-yl)hydrazono)methyl)-phenoxy)ethanone) (9e). Deep brown crystals, yield (0.15 g, 45%), mp <300 °C; IR (KBr) ν 1644 (C=O), 1324, 1498 (NO$_2$) cm^{-1}; MS: MALDI-TOF:

calcd for $[M + H]^+$ $m/z = 931.89$, found 931.04; ^{1}H NMR (DMSO-d$_6$) δ 2.61 (s, 6H, 2CH$_3$), 3.51–3.57 (m, 8H, 4CH$_2$N), 4.50 (s, 4H, 2OCH$_2$), 7.09 (d, $J = 7.5$ Hz, 4H, ArH's), 7.46 (d, $J = 8.1$ Hz, 4H, ArH's), 7.83 (d, $J = 7.8$ Hz, 4H, ArH's), 8.19 (d, $J = 7.8$ Hz, 4H, ArH's), 8.64 (s, 2H, 2CH=N), 11.06 (s, 2H, 2 NH) ppm; ^{13}C NMR (DMSO-d$_6$) δ 16.65, 40.93, 41.43, 43.74, 44.24, 65.92, 113.82, 115.29, 125.78, 126.62, 130.27, 141.03, 142.31, 149.20, 160.78, 161.16, 165.79, 171.40, 178.53. Anal. calcd: for C$_{42}$H$_{38}$N$_{14}$O$_8$S$_2$ (930.98): C, 54.19; H, 4.11; N, 21.06%. Found: C, 54.16; H, 4.26; N, 21.31%.

3.1.4.7 1,1′-(Piperazine-1,4-diyl)bis(2-(2-(((4-methyl-5-(4-tolylazo)thiazol-2-yl)hydrazono)methyl)-phenoxy)ethanone) (9f). Orange crystals, yield (0.1 g, 33%), mp 264–266 °C; IR (KBr) ν 3219 (NH), 1629 (C=O), cm^{-1}; MS: MALDI-TOF: calcd for $[M + H]^+$ $m/z = 870.04$, found 870.37; ^{1}H NMR (DMSO-d$_6$) δ 2.26 (s, 6H, 2CH$_3$Ar), 2.58 (s, 6H, 2CH$_3$), 3.51–3.56 (m, 8H, 4CH$_2$N), 5.06 (s, 4H, 2OCH$_2$), 7.06–7.15 (m, 8H, ArH's), 7.26 (d, 4H, $J = 8.1$ Hz, 4H, ArH's), 7.44–7.65 (m, 2H, ArH's), 7.99 (d, $J = 7.5$ Hz, 2H, ArH's), 8.95 (s, 2H, 2CH=N), 10.54 (s, 2H, 2 NH); ^{13}C NMR (DMSO-d$_6$) δ 16.65, 20.54, 40.99, 41.39, 43.85, 44.25, 66.23, 113.72, 114.42, 121.32, 122.18, 126.49, 129.91, 131.51, 133.23, 137.29, 141.18, 155.21, 157.79, 166.01, 173.19, 178.38 ppm. Anal. calcd: for C$_{44}$H$_{44}$N$_{12}$O$_4$S$_2$ (869.04): C, 60.81; H, 5.10; N, 19.34%. Found: C, 60.62; H, 4.88; N, 19.54%.

3.1.4.8 1,1′-(Piperazine-1,4-diyl)bis(2-(2-(((4-methyl-5-(4-fluorophenylazo)thiazol-2-yl)hydrazono)-methyl)phenoxy)ethanone) (9g). Orange crystals, yield (0.15 g, 48%), mp 266–268 °C; IR (KBr) ν 3213 (NH), 1648 (C=O) cm^{-1}; MS: MALDI-TOF: calcd for $[M + Na]^+$ $m/z = 899.96$, found 899.05; ^{1}H NMR (DMSO-d$_6$) δ 2.58 (s, 6H, 2CH$_3$), 3.51–3.57 (m, 8H, 4 CH$_2$N), 5.06 (s, 4H, 2OCH$_2$), 7.06–7.19 (m, 8H, ArH's), 7.35 (s, 2H, ArH's), 7.46–4.48 (m, 2H, ArH's), 7.65–7.9 (m, 2H, ArH's), 7.98 (d, $J = 7.5$ Hz, 2H, ArH's), 8.96 (s, 2H, 2CH=N), 10.59 (s, 2H, 2 NH); ^{13}C NMR (DMSO-d$_6$) δ 16.66, 41.19, 41.47, 43.92, 44.19, 66.26, 113.70, 115.81, 116.30, 121.35, 122.18, 126.56, 133.31, 137.96, 140.09, 155.46, 156.44, 157.83, 166.05, 173.07, 178.58 ppm. Anal. calcd: for C$_{42}$H$_{38}$F$_2$N$_{12}$O$_4$S$_2$ (876.96): C, 57.52; H, 4.37; N, 19.17%. Found: 57.38; H, 4.44; N, 19.03%.

3.1.4.9 1,1′-(Piperazine-1,4-diyl)bis(2-(2-(((4-methyl-5-(4-chlorophenylazo)thiazol-2-yl)hydrazono)-methyl)phenoxy)ethanone) (9h). Deep red crystals, yield (0.13 g, 41%), mp 280–282 °C; IR (KBr) ν 3217 (NH), 1628 (C=O), cm^{-1}; MS: MALDI-TOF: calcd for $[M + H]^+$ $m/z = 910.87$, found 910.06; 909.01; ^{1}H NMR (DMSO-d$_6$) δ 2.58 (s, 6H, 2CH$_3$), 3.50–3.56 (m, 8H, 4CH$_2$N), 5.06 (s, 4H, 2OCH$_2$), 7.06–7.14 (m, 3H, ArH's), 7.35 (s, 9H, ArH's), 7.46 (t, $J = 7.2$ Hz, 2H, ArH's), 7.98 (d, $J = 7.8$ Hz, 2H, ArH's), 8.96 (s, 2H, 2CH=N), 10.64 (s, 2H, 2NH); ^{13}C NMR (DMSO-d$_6$) δ 16.52, 41.40, 41.67, 43.73, 44.05, 66.22, 113.59, 115.70, 121.12, 122.02, 125.74, 126.39, 129.13, 133.12, 138.61, 142.36, 155.44, 157.72, 165.82, 172.76, 178.40. Anal. calcd: for C$_{42}$H$_{38}$Cl$_{12}$N$_{12}$O$_4$S$_2$ (909.87): C, 55.44; H, 4.21; N, 18.47%. Found: C, 55.32; H, 4.08; N, 18.53%.

3.1.4.10 1,1′-(Piperazine-1,4-diyl)bis(2-(2-(((4-methyl-5-(4-bromophenylazo)thiazol-2-yl)hydrazono)-methyl)phenoxy)ethanone) (9i). Orange crystals, yield (0.13 g, 37%), mp 282–284 °C; IR (KBr) ν 3212 (NH), 1629 (C=O) cm^{-1}; MS: MALDI-TOF: calcd for $[M + H]^+$ $m/z = 999.77$, found 999.04; ^{1}H NMR (DMSO-d$_6$) δ 2.59 (s, 6H, 2CH$_3$), 3.50–3.56 (m, 8H, 4 CH$_2$N), 5.06 (s, 4H, 2OCH$_2$), 7.0–7.14 (m, 4H, ArH's), 7.28–7.31 (m, 4H, ArH's), 7.48 (brs, 6H, ArH's), 7.98 (d, $J = 7.2$ Hz, 2H, ArH's), 8.96 (s, 2H, 2CH=N), 10.65 (s, 2H, 2NH) ppm; ^{13}C NMR (DMSO-d$_6$) δ 16.77, 41.19, 41.44, 43.95, 44.21, 66.40, 113.88, 116.36, 121.39, 122.17, 126.58, 132.25, 133.43, 138.92, 142.96, 155.73, 157.96, 166.04, 172.93, 178.74. Anal. calcd: for C$_{42}$H$_{38}$Br$_2$N$_{12}$O$_4$S$_2$ (998.77): C, 50.51; H, 3.84; N, 16.83%. Found: C, 50.62; H, 3.73; N, 16.92%.

3.1.4.11 1,1′-(Piperazine-1,4-diyl)bis(2-(2-(((4-methyl-5-(4-nitrophenylazo)thiazol-2-yl)hydrazono)-methyl)phenoxy)ethanone) (9j). Dark brown crystals, yield (0.13 g, 40%), mp 240–242 °C; IR (KBr) δ 3196 (NH), 1648 (C=O), 1324, 1485 (NO$_2$) cm^{-1}; MS: MALDI-TOF: calcd for $[M + H]^+$ $m/z = 931.98$, found 931.91; ^{1}H NMR (DMSO-d$_6$) δ 2.62 (s, 6H, 2CH$_3$), 3.50–3.56 (m, 8H, 4 CH$_2$N), 5.06 (s, 4H, 2OCH$_2$), 7.07–7.15 (m, 6H, ArH's), 7.48 (m, 4H, ArH's), 7.98 (d, $J = 7.8$ Hz, 2H, ArH's), 8.19 (brs, 4H, ArH's), 8.98 (s, 2H, 2CH=N), 11.09 (s, 2H, 2 NH) ppm; ^{13}C NMR (DMSO-d$_6$) δ 16.86, 41.29, 41.75, 43.98, 44.50, 66.36, 112.64, 114.04, 121.39, 122.09, 125.91, 126.67, 133.62, 141.25, 142.30, 149.28, 156.56, 158.04, 166.06, 172.53, 179.14. Anal. calcd: for C$_{42}$H$_{38}$N$_{14}$O$_8$S$_2$ (930.98): C, 54.19; H, 4.11; N, 21.06%. Found: C, 54.31; H, 4.23; N, 21.15%.

3.1.4.12 1,1′-(Piperazine-1,4-diyl)bis(2-(4-(((3,5-diphenyl-1,3,4-thiadiazol-2(3H)-ylidene)hydrazono)-methyl)phenoxy)ethanone) (13a). Pale yellow crystals, yield (0.2 g, 63%), mp 214–216 °C; IR (KBr) ν 1604 (C=N), 1658 (C=O), cm^{-1}; MS: MALDI-TOF: calcd for $[M + H]^+$ $m/z = 912.07$, found 912.32; ^{1}H NMR (DMSO-d$_6$) δ 3.50–3.55 (m, 8H, 4 CH$_2$N), 4.95 (s, 4H, 2OCH$_2$), 7.03 (d, $J = 7.5$ Hz, 4H, ArH's), 7.34 (t, $J = 7.8$ Hz, 4H, ArH's), 7.51–7.56 (m, 8H, ArH's), 7.74 (d, $J = 7.5$ Hz, 4H, ArH's), 7.86 (s, 4H, ArH's), 8.10 (d, $J = 7.8$ Hz, 4H, ArH's), 8.43 (s, 2H, 2CH=N). Anal. calcd: for C$_{50}$H$_{42}$N$_{10}$O$_4$S$_2$ (911.07): C, 65.92; H, 4.65; N, 15.37%. Found: C, 65.78; H, 4.48; N, 15.42%.

3.1.4.13 1,1′-(Piperazine-1,4-diyl)bis(2-(4-(((5-(4-chlorophenyl)-3-phenyl-1,3,4-thiadiazol-2(3H)-ylidene)-hydrazono)methyl)phenoxy)ethanone) (13b). Yellow crystals, yield (0.15 g, 43%), mp 260–262 °C; IR (KBr) ν 1607 (C=N), 1660 (C=O) cm^{-1}; MS: MALDI-TOF: calcd for $[M + H]^+$ $m/z = 980.96$, found 980.04; ^{1}H NMR (DMSO-d$_6$) δ 3.50–3.57 (m, 8H, 4CH$_2$N), 4.96 (s, 4H, 2OCH$_2$), 7.03 (d, $J = 8.4$ Hz, 4H, ArH's), 7.34 (t, $J = 7.5$ Hz, 2H, ArH's), 7.34 (t, $J = 7.5$ Hz, 4H, ArH's), 7.61 (d, $J = 8.4$ Hz, 4H, ArH's), 7.74 (d, $J = 8.4$ Hz, 4H, ArH's), 7.88 (d, $J = 8.4$ Hz, 4H, ArH's), 8.09 (d, $J = 8.4$ Hz, 4H, ArH's), 8.44 (s, 2H, 2CH=N); ^{13}C NMR (DMSO-d$_6$) δ 40.99, 41.41, 43.80, 44.05, 66.06, 115.32, 121.93, 126.54, 127.53, 128.17, 128.66, 129.25, 129.66, 135.89, 139.48, 149.30, 154.75, 160.19, 164.28, 166.13 ppm. Anal. calcd: for C$_{50}$H$_{40}$Cl$_2$N$_{10}$O$_4$S$_2$ (979.96): C, 61.28; H, 4.11; N, 14.29%. Found: C, 61.35; H, 4.23; N, 14.04%.

3.1.4.14 1,1′-(Piperazine-1,4-diyl)bis(2-(2-(((3,5-diphenyl-1,3,4-thiadiazol-2(3H)-ylidene)hydrazono)-methyl)phenoxy)ethanone) (13c). Yellow crystals, yield (0.14 g, 44%), mp 144–146 °C; IR (KBr) ν 1602 (C=N), 1659 (C=O) cm^{-1} MS: MALDI-TOF: calcd for $[M + H]^+$ $m/z = 912.07$, found 912.21; ^{1}H NMR (DMSO-d$_6$) δ 3.50–3.56 (m, 8H, 4CH$_2$N), 5.01 (s, 4H, 2OCH$_2$), 7.03–7.09 (m, 6H, ArH's), 7.31–7.42 (m, 6H, ArH's), 7.42–7.57 (m, 6H, ArH's), 7.88 (brs, 4H, ArH's), 7.94 (d, $J = 7.8$ Hz, 2H,

ArH's), 8.10 (d, J = 8.1 Hz, 4H, ArH's), 8.77 (s, 2H, 2CH=N). Anal. calcd: for $C_{50}H_{42}N_{10}O_4S_2$ (911.07): C, 65.92; H, 4.65; N, 15.37%. Found: C, 65.78; H, 4.44; N, 15.45%.

3.1.4.15 1,1′-(Piperazine-1,4-diyl)bis(2-(2-(((5-(4-chlorophenyl)-3-phenyl-1,3,4-thiadiazol-2(3H)-ylidene)-hydrazono) methyl)phenoxy)ethanone) (13d). Yellow crystals, yield (0.1 g, 29%), mp 278–280 °C; IR (KBr) ν 1604 (C=N), 1667 (C=O) cm^{-1}; MS: MALDI-TOF: calcd for $[M + H1]^+$ m/z = 980.96, found 980.96; ^{1}H NMR (DMSO-d$_6$) δ 3.49–3.55 (m, 8H, 4CH$_2$N), 5.0 (s, 4H, 2OCH$_2$), 7.02–7.09 (m, 4H, ArH's), 7.31–7.42 (m, 4H, ArH's), 7.53 (t, J = 7.2 Hz, 4H, ArH's), 7.60 (d, J = 7.8 Hz, 4H, ArH's), 7.87–7.93 (m, 6H, ArH's), 8.08 (d, J = 7.8 Hz, 4H, ArH's), 8.76 (s, 2H, 2CH=N). Anal. calcd for $C_{50}H_{40}Cl_{12}N_{10}O_4S_2$ (979.96): C, 61.28; H, 4.11; N, 14.29%. Found: C, 61.12; H, 4.23; N, 14.11%.

3.1.5. Synthesis of the piperazine-based bis-thiazole hybrids 15a–h

3.1.5.1 General procedure. The bis-thiosemicarbazone **7a** or **7b** (0.278 g, 0.5 mmol), were mixed with the appropriate α-bromocarbonyl compounds **14a–e** (1.0 mmol) in dry EtOH/DMF (1 : 3, 10 mL), then heated at reflux condition for 8 hours, during which triethylamine (0.1 mL) was added. The reaction vessel was left to cool to ambient temperature, and the isolated solid product was collected by filtration, washed with ethanol, and dried. Purification of the crude products by recrystallization from EtOH/DMF mixed solvents produced the corresponding bis-thiazole derivatives **15a–h**, respectively.

3.1.5.2 1,1′-(Piperazine-1,4-diyl)bis(2-(4-(((4-phenylthiazol-2(3H)-ylidene)hydrazineylidene)methyl)-phenoxy)ethanone) (15a). Yellow crystals, yield (0.13 g, 48%), mp 262–264 °C; IR (KBr) ν 3292 (NH), 1670 (C=O), 1605 (C=N) cm^{-1}; MS: MALDI-TOF: calcd for $[M + H]^+$ m/z = 757.90, found 757.14; ^{1}H NMR (DMSO-d$_6$) δ 3.49–3.56 (m, 8H, 4NCH$_2$), 4.92 (s, 4H, 2OCH$_2$), 7.0 (d, J = 8.7 Hz, 4H, ArH's), 7.28–7.31 (m, 4H, thiazole-2-CH, 2ArH's), 7.39 (t, J = 7.8 Hz, 4H, ArH's), 7.59 (d, J = 8.4 Hz, 4H, ArH's), 7.84 (d, J = 8.1 Hz, 4H, ArH's), 7.86 (s, 2H, 2CH=N), 11.99 (s, 2H, 2NH) ppm; ^{13}C NMR (DMSO-d$_6$) δ 41.18, 41.40, 44.03, 44.53, 66.03, 94.41, 103.49, 115.18, 125.61, 127.53, 127.75, 128.71, 134.83, 141.25, 150.60, 159.12, 166.02, 168.45 ppm. Anal. calcd: for $C_{40}H_{36}N_8O_4S_2$ (756.90): C, 63.47; H, 4.79; N, 14.80%. Found: C, 63.72; H, 4.76; N, 14.69%.

3.1.5.3 1,1′-(Piperazine-1,4-diyl)bis(2-(4-(((4-(4-methoxyphenyl)thiazol-2(3H)-ylidene)hydrazineylidene)-methyl)phenoxy) ethanone) (15b). Dark brown crystals, yield (0.13 g, 44%), mp 260–262 °C; IR (KBr) ν 3297 (NH), 1653 (C=O), 1604 (C=N) cm^{-1}; MS: MALDI-TOF: calcd for $[M + H]^+$ m/z = 817.95, found 817.22; ^{1}H NMR (DMSO-d$_6$) δ 3.50–3.56 (m, 8H, 4CH$_2$N), 3.75 (s, 6H, 2CH$_3$O), 4.92 (s, 4H, 2OCH$_2$), 6.96 (d, J = 8.7 Hz, 4H, ArH's), 7.0 (d, J = 8.7 Hz, 4H, ArH's), 7.1 (s, 2H, thiazole-2-CH), 7.59 (d, J = 8.7 Hz, 4H, ArH's), 7.77 (d, J = 8.4 Hz, 4H, ArH's), 7.98 (s, 2H, 2CH=N), 11.95 (br, 2H, 2NH); ^{13}C NMR (DMSO-d$_6$) δ 41.06, 41.31, 43.87, 44.37, 55.09, 65.83, 101.22, 113.94, 115.05, 126.84, 127.45, 127.62, 141.03, 150.31, 154.34, 158.74, 158.97, 165.93, 168.24. Anal. calcd: for $C_{42}H_{40}N_8O_6S_2$ (816.95): C, 61.75; H, 4.94; N, 13.72%. Found: C, 61.88; H, 4.78; N, 13.55.

3.1.5.4 1,1′-(Piperazine-1,4-diyl)bis(2-(4-(((4-(4-chlorophenyl)thiazol-2(3H)-ylidene)hydrazineylidene)-methyl)phenoxy)

ethanone) (15c). Pale yellow crystals, yield (0.12 g, 41%), mp 278–280 °C; IR (KBr) ν 3181 (NH), 1660 (C=O), 1607 (C=N) cm^{-1}; MS: MALDI-TOF: calcd for $[M + H]^+$ m/z = 826.78, found 826.20; ^{1}H NMR (DMSO-d$_6$) δ 3.50–3.56 (m, 8H, 4CH$_2$N), 4.93 (s, 4H, 2OCH$_2$), 7.01 (d, J = 7.8 Hz, 4H, ArH's), 7.35 (s, 2H, thiazole-2-CH), 7.45 (d, J = 8.1 Hz, 4H, ArH's), 7.59 (d, J = 8.1 Hz, 4H, ArH's), 7.86 (d, J = 7.5 Hz, 4H, ArH's), 7.99 (s, 2H, 2CH=N), 12.0 (s, 2H, 2 NH); ^{13}C NMR (DMSO-d$_6$) δ 41.05, 41.35, 43.87, 44.20, 65.88, 104.18, 115.05, 127.19, 127.34, 127.68, 128.61, 131.88, 133.57, 141.31, 149.27, 159.03, 165.89, 168.47. Anal. calcd for $C_{40}H_{34}Cl_2N_8O_4S_2$ (825.78): C, 58.18; H, 4.15; N, 13.57%. Found: C, 58.34; H, 4.27; N, 13.27%.

3.1.5.5 1,1′-(Piperazine-1,4-diyl)bis(2-(4-(((4-(4-bromophenyl) thiazol-2(3H)-ylidene)hydrazineylidene)-methyl)phenoxy) ethanone) (15d). Pale yellow solid, yield (0.16 g, 50%), mp 288–290 °C; IR (KBr) ν 3292 (NH), 1660 (C=O), 1606 (C=N) cm^{-1}; ^{1}H NMR (DMSO-d$_6$) δ 3.49–3.55 (m, 8H, 4 CH$_2$N), 4.92 (s, 4H, 2OCH$_2$), 7.0 (d, J = 7.2 Hz, 4H, ArH's), 7.35 (s, 2H, thiazole-2-CH), 7.45 (d, J = 8.1 Hz, 4H, ArH's), 7.59 (d, J = 7.8 Hz, 4H, ArH's), 7.85 (d, J = 8.1 Hz, 4H, ArH's), 7.99 (s, 2H, 2CH=N), 11.99 (s, 2H, 2 NH). ^{13}C NMR (DMSO-d$_6$) δ 40.81, 41.41, 43.98, 44.58, 65.91, 104.31, 115.16, 127.31, 127.78, 128.72, 131.98, 133.68, 141.44, 149.38, 159.14, 166.01, 168.57. Anal. calcd: for $C_{40}H_{34}Br_2N_8O_4S_2$ (914.69): C, 52.52; H, 3.75; N, 12.25%. Found: C, 52.41; H, 3.88; N, 12.11%.

3.1.5.6 1,1′-(Piperazine-1,4-diyl)bis(2-(4-(((4-(coumarin-3-yl) thiazol-2(3H)-ylidene)hydrazineylidene)-methyl)phenoxy) ethanone) (15e). Yellow solid, yield (0.18 g, 56%), mp 320–322 °C; IR (KBr) ν 3230 (NH), 1713, 1662 (2C=O), 1605 (C=N) cm^{-1}; MS: MALDI-TOF: calcd for $[M + H]^+$ m/z = 893.96, found 893.00; ^{1}H NMR (DMSO-d$_6$) δ 3.49–3.56 (m, 8H, 4CH$_2$N), 4.93 (s, 4H, 2OCH$_2$), 7.01 (d, J = 8.4 Hz, 4H, ArH's), 7.36–7.46 (m, 4H, ArH's), 7.59–7.65 (m, 6H, ArH's), 7.75 (s, 2H, thiazole-2-CH), 7.85 (d, J = 7.8 Hz, 2H, ArH's), 8.01 (s, 2H, ArH's), 8.54 (s, 2H, 2CH=N), 12.03 (s, 2H, 2NH) ppm. Anal. calcd: for $C_{46}H_{36}N_8O_8S_2$ (892.96): C, 61.87; H, 4.06; N, 12.55%. Found: C, 61.95; H, 4.21; N, 12.38%.

3.1.5.7 1,1′-(Piperazine-1,4-diyl)bis(2-(2-(((4-(4-chlorophenyl) thiazol-2(3H)-ylidene)hydrazineylidene)-methyl)phenoxy) ethanone) (15f). Yellow crystals, yield (0.18 g, 62%), mp 208–210 °C; IR (KBr) ν 3191 (NH), 1659 (C=O), 1602(C=N) cm^{-1}; MS: MALDI-TOF: calcd for $[M + H]^+$ m/z = 826.78, found 826.18; ^{1}H NMR (DMSO-d$_6$) δ 3.53–3.57 (m, 8H, 4 NCH$_2$), 4.99 (s, 4H, 2OCH$_2$), 6.70–7.04 (m, 4H, ArH's), 7.31 (d, J = 7.8 Hz, 2H, ArH's), 7.36 (s, 2H, thiazole-2-CH), 7.45 (d, J = 8.7 Hz, 4H, ArH's), 7.80 (d, J = 8.1 Hz, 2H, ArH's), 7.85 (d, J = 8.4 Hz, 4H, ArH's), 8.42 (s, 2H, 2CH=N), 12.18 (s, 2H, 2NH); ^{13}C NMR (DMSO-d$_6$) δ 41.13, 41.41, 44.02, 44.27, 66.20, 104.39, 112.96, 121.20, 122.72, 125.01, 127.25, 128.66, 130.49, 131.97, 133.58, 137.04, 149.38, 155.90, 165.96, 168.48. Anal. calcd: for $C_{40}H_{34}Cl_2N_8O_4S_2$ (825.78): C, 58.18; H, 4.15; N, 13.57%. Found: C, 58.32; H, 4.22; N, 13.48%.

3.1.5.8 1,1′-(Piperazine-1,4-diyl)bis(2-(2-(((4-(4-bromophenyl) thiazol-2(3H)-ylidene)hydrazineylidene)-methyl)phenoxy) ethanone) (15g). Yellow crystals, yield (0.14 g, 44%), mp 218–220 °C; IR (KBr) ν 3196 (NH), 1642 (C=O), 1601 (C=N) cm^{-1}; ^{1}H

NMR (DMSO-d$_6$) δ 3.53–3.56 (m, 8H, 4CH$_2$N), 4.99 (s, 4H, 2OCH$_2$), 6.99–7.02 (m, 4H, ArH's), 7.31 (d, J = 7.8 Hz, 2H, ArH's), 7.37 (s, 2H, thiazole-2-CH), 7.45 (d, J = 7.5 Hz, 4H, ArH's), 7.79 (d, J = 7.8 Hz, 2H, ArH's), 7.86 (d, J = 7.5 Hz, 4H, ArH's), 8.42 (s, 2H, 2CH=N), 12.18 (s, 2H, 2 NH); ^{13}C NMR (DMSO-d$_6$) δ 41.14, 41.44, 44.05, 44.29, 66.36, 104.39, 112.96, 121.18, 122.71, 124.99, 127.24, 128.63, 130.46, 131.93, 133.57, 137.04, 149.34, 155.88, 165.95, 168.43. Anal. calcd: for C$_{40}$H$_{34}$Br$_2$N$_8$O$_4$S$_2$ (914.69): C, 52.52; H, 3.75; N, 12.25%. Found: C, 52.45; H, 3.88; N, 12.12%.

3.1.5.9 1,1′-(Piperazine-1,4-diyl)bis(2-(2-(((4-(coumarin-3-yl) thiazol-2(3H)-ylidene)hydrazineylidene)-methyl)phenoxy) ethanone) (15h). Brown crystals, yield (0.16 g, 50%), mp 198–200 °C; IR (KBr) ν 3200 (NH), 1650, 1713 (2C=O), 1603 (C= N) cm^{-1}; MS: MALDI-TOF: calcd for [M + H]$^+$ m/z = 893.96, found 893.17; ^{1}H NMR (DMSO-d$_6$) δ 3.44–3.54 (m, 8H, 4 NCH$_2$), 5.01 (s, 4H, 2OCH$_2$), 7.02–7.04 (m, 4H, ArH's), 7.31–7.45 (m, 6H, ArH's), 7.59–7.64 (m, 2H, ArH's), 7.73 (s, 2H, thiazole-2-CH), 7.75–7.84 (m, 4H, ArH's), 8.45 (s, 2H, ArH's), 8.51 (s, 2H, 2CH=N), 12.21 (s, 2H, 2 NH). Anal. calcd: for C$_{46}$H$_{36}$N$_8$O$_8$S$_2$ (892.96): C, 61.87; H, 4.06; N, 12.55%. Found: 61.72; H, 4.21; N, 12.32%.

3.2. Biological evaluation

3.2.1 Cytotoxicity against cancer cells

3.2.1.1 Drugs and chemicals. The samples were dissolved in DMSO to yield a stock solution of 2 mg mL^{-1} and serially diluted in DMEM (Dulbecco's Modified Eagle Medium) supplemented medium immediately before use to yield concentrations ranging between 0–50 μg mL^{-1} for the human colon carcinoma (HCT116), human liver carcinoma (HEPG2), human breast carcinoma (MCF7) and human dermal normal (HDF) cell lines. The final concentration of DMSO never exceeded 0.1% (v/v) in control and treated samples to avoid potential toxicity to the cell lines that could lead to cell death.

3.2.1.2 Human cancer cell lines. Human carcinoma (HCT116, HEPG2, and MCF7) cell lines and human normal dermal cell lines (HDF) were obtained from the National Cancer Institute, Cairo University, Egypt. The tumor cell line was maintained as monolayer cultures in DMEM supplemented with 10% FBS and 1% penicillin–streptomycin.

3.2.1.3 Cytotoxicity using SRB assay. The percentage of cell growth inhibition at the single dose [100 μM] and cytotoxicity (IC$_{50}$) were determined using the sulforhodamine-B (SRB) method[69,70] on both normal skin (HDF) cell line and the cancer cell lines: HCT116, HEPG2, and MCF7. This was done at the beginning of the study to determine a single dose % inhibition at 100 μM for the compounds to select the most effective ones among them as anti-cancer agents. Then, the cytotoxicity of the drugs on the malignant cell line compared to the normal cell line was evaluated. Cells were treated for 48 h with different concentrations (0, 6.25, 12.5, 25, and 50 μM) of compounds selected. The optical density (OD) was measured spectrophotometrically at 570 nm using an ELISA microplate reader (Sunrise TM, TECAN, Germany). The mean values were estimated as the percentage of cell viability as follows:

$$\% \text{ Cell viability} = \frac{\text{OD(treated cells)}}{\text{OD(control cells)}} \times 100$$

The IC$_{50}$ value of each drug was calculated using dose–response curve-fitting models (Graph-Pad Prism software, version, 8). The concentration of IC$_{50}$ was used for further treatment to do other molecular pathways.

3.2.2 EGFR kinase inhibitory assay.
Compounds **7a**, **9a**, **9b**, and **9i** were evaluated for the EGFR kinase inhibition using "Catalog #40321". They were dissolved in DMSO (0.1%), and four serial concentrations were prepared following the manufacturer's instructions.[72]

3.2.3 Investigation of apoptosis

3.2.3.1 Annexin V/PI staining and cell cycle analysis. HCT-116 cells were seeded into 6-well culture plates (3–5 × 10^5 cells per well) and incubated overnight. Cells were treated with compound **9i** at their IC$_{50}$ values for 48 h. Next, media supernatants and cells were collected and rinsed with ice-cold PBS. Then, cells were suspended the cells in 100 μL of annexin binding buffer solution "1.4 M NaCl, 25 mM CaCl$_2$, and 0.1 M Hepes/NaOH, pH 7.4" and incubated with "Annexin V-FITC solution (1 : 100) and propidium iodide (PI)" at a concentration equals 10 μM in the dark for 30 min. Stained cells were then acquired by Cytoflex from Beckham Coulter Flow Cytometer with cytexpert software.[73–76]

3.2.3.2 Real time-polymerase chain reaction for the selected genes. Gene expression of Bcl-2, the anti-apoptotic gene, and the pro-apoptotic genes P53, PUMA, and caspases-3,8,9 were evaluated to delve deeper into the apoptotic pathway. HCT-116 cells were treated with compound **9i** at their IC$_{50}$ values for 48 h. After treatment, the RT-PCR reaction was carried out following routine work. Then, the C_t values were collected to calculate the relative genes' expression in all samples by normalization to the β-actin housekeeping gene.[73,77]

4. Conclusion

Convenient synthetic routes for constructing some novel bis-thiazoles and bis-1,3,4-thiadiazoles linked to piperazine core were reported in good outcomes. The easy synthesis of the target compounds in good yields under mild reaction conditions in a short reaction time utilizing affordable starting materials was one of these reactions' benefits. Another advantage was that simple crystallization could easily isolate the desired compounds without chromatographic purification. The anti-cancer activity of synthesized compounds was assessed, and the results showed promising results of bis-thiazoles **9a** and **9i** against HCT116 cell lines. Interestingly, compound **9i** had potent EGFR kinase inhibition with an IC$_{50}$ value of 1.2 nM with inhibition of 97.5% compared to Erlotinib (IC$_{50}$ = 1.3 nM, 97.8% inhibition). Moreover, compound **9i** significantly induced apoptosis in HCT-16 cells by 4.16-fold by having 16.85% total apoptosis in treated cells compared to 4.05% for control moreover, arresting the cell cycle at the P2 phase. A promising EGFR-targeted chemotherapeutic drug for the treatment of colon cancer, compound **9i** was thus verified.

Data availability

All data associated with this manuscript will be available upon reasonable request from the corresponding author

Conflicts of interest

There are no conflicts to declare.

References

1 K. E. Gettys, Z. Ye and M. Dai, *Synthesis*, 2017, **49**, 2589–2604.

2 C. C. Guo, H.-P. Li and X.-B. Zhang, *Bioorg. Med. Chem.*, 2003, **11**, 1745–1751.

3 C. C. Guo, R.-B. Tong and K.-L. Li, *Bioorg. Med. Chem.*, 2004, **12**, 2469–2475.

4 E. Vitaku, D. T. Smith and J. T. Njardarson, *J. Med. Chem.*, 2014, **57**, 10257–10274.

5 M. Rizwan, S. Noreen, S. Asim, Z. Liaqat, M. Shaheen and H. Ibrahim, *Chem. Inorg. Mater.*, 2024, **2**, 100041.

6 M. Shaquiquzzaman, G. Verma, A. Marella, M. Akhter, W. Akhtar, M. F. Khan, S. Tasneem and M. M. Alam, *Eur. J. Med. Chem.*, 2015, **102**, 487–529.

7 N. A. Meanwell and O. Loiseleur, *J. Agric. Food Chem.*, 2022, **70**, 10942–10971.

8 P. Meena, V. Nemaysh, M. Khatri, A. Manral, P. M. Luthra and M. Tiwari, Synthesis, *Bioorg. Med. Chem.*, 2015, **23**, 1135–1148.

9 L. Yurtta, Z. A. Kaplancikli and Y. Ozkay, *J. Enzyme Inhib. Med. Chem.*, 2013, **28**, 1040–1047.

10 R. S. Upadhayaya, N. Sinha, S. Jain, N. Kishore, R. Chandra and S. K. Arora, *Bioorg. Med. Chem.*, 2004, **12**, 2225–2238.

11 P. Chaudhary, R. Kumar and A. K. Verma, *Bioorg. Med. Chem.*, 2006, **14**, 1819–1826.

12 F. Stegmeier, M. Warmuth, W. R. Sellers and M. Dorsch, *Clin. Pharmacol. Ther.*, 2010, **87**, 543–552.

13 P. W. Manley, F. Blasco, J. Mestan and R. Aichholz, *Bioorg. Med. Chem.*, 2013, **21**, 3231–3239.

14 W. Sneader, C. Hansch, P. Sammnes and J. Taylor, *Comprehensive Medicinal Chemistry*, Pergamon Press, London, 1990, 1, pp. 65–70.

15 R. Aggarwal and G. Sumran, *Eur. J. Med. Chem.*, 2020, **205**, 112652.

16 T. M. Davis, T.-Y. Hung, I.-K. Sim, H. A. Karunajeewa and K. F. Ilett, *Drugs*, 2005, **65**, 75–87.

17 R.-H. Zhang, H.-Y. Guo, H. Deng, J. Li, Z.-S. Quan and J. Enzyme Inhib, *Med. Chem.*, 2021, **36**, 1165–1197.

18 R. Wang, A. M. Piggott, Y.-H. Chooi and H. Li, *Nat. Prod. Rep.*, 2023, **40**, 387–411.

19 P. C. Sharma, K. K. Bansal, A. Sharma, D. Sharma and A. Deep, *Eur. J. Med. Chem.*, 2020, **188**, 112016.

20 A. Petrou, M. Fesatidou and A. Geronikaki, *Molecules*, 2021, **26**, 3166.

21 A. Ayati, S. Emami, S. Moghimi and A. Foroumadi, *Future Med. Chem.*, 2019, **11**, 1929.

22 M. T. Chhabria, S. Patel, P. Modi and P. S. Brahmkshatriya, *Curr. Top. Med. Chem.*, 2016, **16**, 2841.

23 A. B. Muhsinah, M. M. Alharbi, N. A. Kheder, S. M. Soliman, H. A. Ghabbour and Y. N. Mabkhot, *J. Mol. Struct.*, 2024, **1316**, 139083.

24 P. Franchetti, L. Cappellacci, M. Grifantini, A. Barzi, G. Nocentini, H. Yang, A. O'Connor, H. N. Jayaram, C. Carrell and B. M. Goldstein, *J. Med. Chem.*, 1995, **38**, 3829.

25 X. Li, Y. He, C. H. Ruiz, M. Koenig and M. D. Cameron, *Drug Metab. Dispos.*, 2009, **37**, 1242.

26 S. Hu-Lieskovan, S. Mok, B. Homet Moreno, J. Tsoi, L. Robert, L. Goedert, E. M. Pinheiro, R. C. Koya, T. G. Graeber, B. Comin-Anduix and A. Ribas, *Sci. Transl. Med.*, 2015, **18**, 279.

27 K. M. Dawood, T. M. Eldebss, H. S. El-Zahabi, M. H. Yousef and P. Metz, *Eur. J. Med. Chem.*, 2013, **70**, 740–749.

28 K. M. Dawood and S. M. Gomha, *J. Heterocycl. Chem.*, 2015, **52**, 1400–1405.

29 K. M. Dawood and T. A. Farghaly, *Expert Opin. Ther. Pat.*, 2017, **27**, 477–505.

30 S. M. Gomha, M. R. Abdelaziz, N. A. Kheder, H. M. Abdel-Aziz, S. Alterary and Y. N. Mabkhot, *Chem. Cent. J.*, 2017, **11**, 105.

31 S. M. Gomha, N. A. Kheder, M. R. Abdelaziz, Y. N. Mabkhot and A. M. Alhajoi, *Chem. Cent. J.*, 2017, **11**, 25.

32 X. H. Yang, Q. Wen, T. T. Zhao, J. Sun, X. Li, M. Xing, X. Lu and H. L. Zhu, *Bioorg. Med. Chem.*, 2012, **20**, 1181–1187.

33 H. Rajak, A. Agarawal, P. Parmar, B. S. Thakur, R. Veerasamy, P. C. Sharma and M. D. Kharya, *Bioorg. Med. Chem. Lett.*, 2011, **21**, 5735–5738.

34 Q. Ma, W. Ding, Z. Chen and Z. Ma, *Nat. Prod. Res.*, 2018, **32**, 761–766.

35 B. Li, G. Chen, J. Bai, Y. K. Jing and Y. H. Pei, *J. Asian Nat. Prod. Res.*, 2011, **13**, 1146–1150.

36 L. Zhang, L. H. Wang, Y. F. Yang, S. M. Yang, J. H. Zhang and C. H. Tan, *Nat. Prod. Res.*, 2011, **25**, 1676–1679.

37 M. S. Abdelfattah, K. Toume, F. Ahmed, S. K. Sadhu and M. Ishibashi, *Chem. Pharm. Bull.*, 2010, **58**, 1116–1118.

38 A. V. Pakhomova, V. E. Nebolsin, O. V. Pershina, V. A. Krupin, L. A. Sandrikina, E. S. Pan, N. N. Ermakova, O. E. Vaizova, D. Widera, W. D. Grimm and V. Y. E. Kravtsov, *Int. J. Mol. Sci.*, 2020, **21**, 991.

39 J. Han, H. W. Lee, Y. Jin, D. B. Khadka, S. Yang, X. Li, M. Kim and W. J. Cho, *Eur. J. Med. Chem.*, 2020, **188**, 112031.

40 S. Yang, K. R. Jyothi, S. Lim, T. G. Choi, J. H. Kim, S. Akter, M. Jang, H. J. Ahn, H. Y. Kim, M. P. Windisch, D. B. Khadka, C. Zhao, Y. Jin, I. Kang, J. Ha, B. C. Oh, M. Kim, S. S. Kim and W. J. Cho, *J. Med. Chem.*, 2015, **58**, 9546–9561.

41 A. H. Rezayan, S. Hariri, P. Azerang, G. Ghavami, I. Portugal and S. Sardari, *Iran. J. Pharm. Res.*, 2017, **16**, 745–755.

42 K. Singh, S. Banerjee and A. K. Patra, *RSC Adv.*, 2015, **5**, 107503–107513.

43 M. I. El-Gamal, M. S. Abdel-Maksoud, M. M. G. El-Din, K. H. Yoo, D. Baek and C. H. Oh, *Arch. Pharm.*, 2014, **347**, 635–641.

44 M. S. Ayoup, M. A. Fouad, H. Abdel-Hamid, E.-S. Ramadan, M. M. Abu-Serie, A. Noby and M. Teleb, *Eur. J. Med. Chem.*, 2020, **186**, 111875.

45 M. P. Gajewski, H. Beall, M. Schnieder, S. M. Stranahan, M. D. Mosher, K. C. Rider and N. R. Natale, *Bioorg. Med. Chem. Lett.*, 2009, **19**, 4067–4069.

46 Y. Ling, Z. Wang, H. Zhu, X. Wang, W. Zhang, X. Wang, L. Chen, Z. Huang and Y. Zhang, *Bioorg. Med. Chem.*, 2014, **22**, 374–380.

47 H. A. Abdel-Aziz, H. S. El-Zahabi and K. M. Dawood, *Eur. J. Med. Chem.*, 2010, **45**, 2427–2432.

48 K. M. Dawood, H. Abdel-Gawad, H. A. Mohamed and F. A. Badria, *Med. Chem. Res.*, 2011, **20**, 912–919.

49 K. M. Dawood, M. A. Raslan, A. A. Abbas, B. E. Mohamed, M. H. Abdellattif, M. S. Nafie and M. K. Hassan, *Front. Chem.*, 2021, **9**, 694870.

50 F. M Thabet, K. M. Dawood, E. A. Ragab, M. S. Nafie and A. A. Abbas, *RSC Adv.*, 2022, **12**, 23644–23660.

51 K. M. Dawood, M. A. Raslan, A. A. Abbas, B. E. Mohamed and M. S. Nafie, *Anti-Cancer Agents Med. Chem.*, 2023, **23**, 328–345.

52 A. A. Abbas and K. M. Dawood, *Expert Opin. Drug Discovery*, 2022, **17**, 1357–1376.

53 M. E. Salem, E. M. Mahrous, E. A. Ragab, M. S. Nafie and K. M. Dawood, *MBC Chem.*, 2023, **17**(51), 1–17.

54 M. E. Salem, E. M. Mahrous, E. A. Ragab, M. S. Nafie and K. M. Dawood, *ACS Omega*, 2023, **8**, 35359–35369.

55 M. S. Nafie, S. H. Kahwash, M. M. Youssef and K. M. Dawood, *Arch. Pharm.*, 2024, e2400225.

56 A. A. Abbas, T. A. Farghaly and K. M. Dawood, *RSC Adv.*, 2024, **14**, 19752–19779.

57 K. M. Dawod and A. A. Abbas, *ChemistrySelect*, 2021, **6**, 279–305.

58 M. A. El-Atawy, A. Z. Omar, M. Hagar and E. M. Shashira, *Green Chem. Lett. Rev.*, 2019, **12**, 364–376.

59 S. Bondock, T. Albarqi, M. Abboud, T. Nasr, N. M. Mohamed and M. M. Abdou, *RSC Adv.*, 2023, **13**, 24003–24022.

60 W. Dieckmann and O. Platz, *Chem. Ber.*, 1906, **38**, 2989–2995.

61 R. Wodtke, J. Steinberg, M. Köckerling, R. Löser and C. Mamat, *RSC Adv.*, 2018, **8**, 40921–40933.

62 N. F. Eweiss and A. Osman, *J. Heterocycl. Chem.*, 1980, **17**, 1713–1717.

63 M. M. El-Abadelah, A. Q. Hussein and B. A. Thaher, *Heterocycles*, 1991, **32**, 1879–1895.

64 P. Wolkoff, *Can. J. Chem.*, 1975, **53**, 1333–1335.

65 Y. C. Tian, J. K. Li, F. G. Zhang and J. A. Ma, *Adv. Synth. Catal.*, 2021, **363**, 2093–2097.

66 R. M. Cowper and L. H. Davidson, *Org. Synth.*, 1943, **2**, 480.

67 R. B. Mohan and N. G. Reddy, *Synth. Commun.*, 2013, **43**, 2603–2614.

68 C. F. Koelsch, *J. Am. Chem. Soc.*, 1950, **72**, 2993–2995.

69 P. Skehan, R. Storeng, D. Scudiero, A. Monks, V. D. McMahon, J. T. Warren, H. Bokesch, S. Kenney and M. R. Boyd, *J. Natl. Cancer Inst.*, 1990, **82**, 1107.

70 M. Sharaky, M. Kamel, M. A. Aziz, M. Omran, M. M. Rageh, K. A. Abouzid and S. A. Shouman, *J. Enzyme Inhib. Med. Chem.*, 2020, **35**, 1641–1656.

71 M. E. Salem, I. M. Fares, S. A. Ghozlan, M. M. Abdel-Aziz, I. A. Abdelhamid and A. H. M. Elwahy, *J. Heterocycl. Chem.*, 2022, **59**, 1907–1926.

72 J. L. Nakamura, *Expert Opin. Ther. Targets*, 2007, **11**, 463–472.

73 M. S. Nafie, K. Arafa, N. K. Sedky, A. A. Alakhdar and R. K. Arafa, *Chem.-Biol. Interact.*, 2020, **324**, 109087.

74 M. S. Nafie, A. M. Amer, A. K. Mohamed and E. S. Tantawy, *Bioorg. Med. Chem.*, 2020, **28**, 115828.

75 E. M. Gad, M. S. Nafie, E. H. Eltamany, M. S. A. G. Hammad, A. Barakat and A. T. A. Boraei, *Molecules*, 2020, **25**, 2523.

76 M. S. Nafie, S. M. Kishk, S. Mahgoub and A. M. Amer, *Chem. Biol. Drug Des.*, 2022, **99**, 547–560.

77 M. S. Nafie, S. Mahgoub and A. M. Amer, *Chem. Biol. Drug Des.*, 2021, **97**, 553–564.